Atropisomerism: A Pharmaceutical and Process Perspective

Blake Ocampo

October 31, 2023

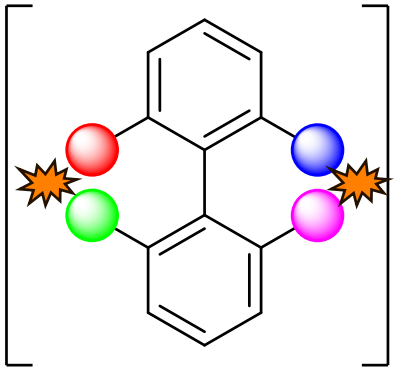

The Discovery of Atropisomerism

Leading Hypothesis: Planar

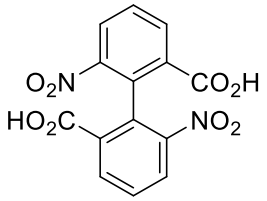

trans

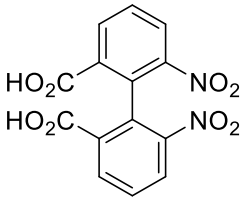

cis

Kaufler Hypothesis: Stacked

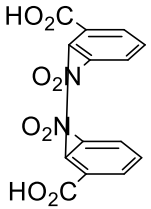

trans

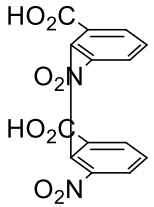

cis

- Both the *cis* and *trans* forms of the leading hypothesis are symmetrical
- The *trans* form of the Kaufler hypothesis should be optically active

Resolution of Both Salts

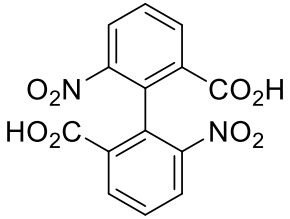

mp = 263 °C
optically inactive

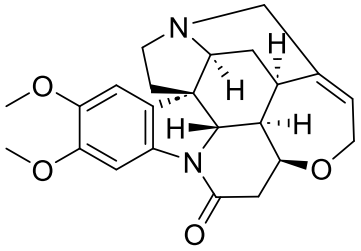

fractional crystallization in H_2O,
then H_2SO_4 to each salt

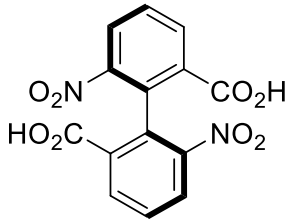

mp = 230-231 °C
$[\alpha]_d$ = +225.3°

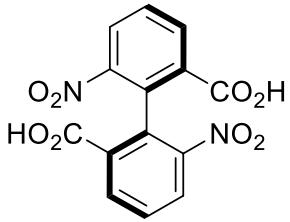

mp = 230-238 °C
$[\alpha]_d$ = -169.7°

- Both compounds isolated were optically active
- Suggested the aryl rings were perpendicular to each other

Christie, G. H.; Kenner, J. *J. Chem. Soc., Trans.* **1922**, *121*, 614–620.

Defining Atropisomers

The Classic Definition:

Atropisomer: a subclass of isolable conformers which arise from hindered rotation about a single bond

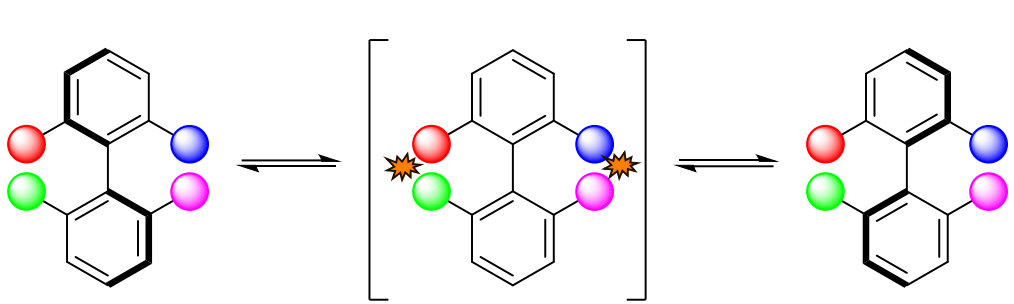

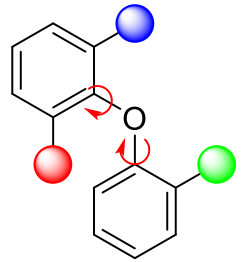

diaryl ethers

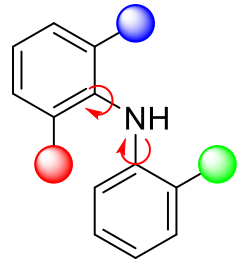

diaryl amines

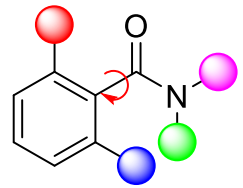

benzamides

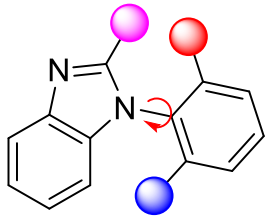

heterobiaryls

What about Axial Chirality?

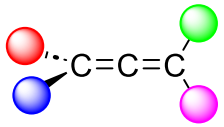

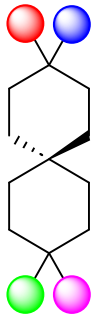

Despite axial chirality, allenes and spiranes are not atropisomers

Assigning Stereochemistry

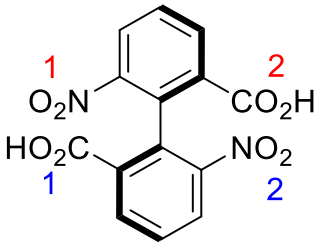

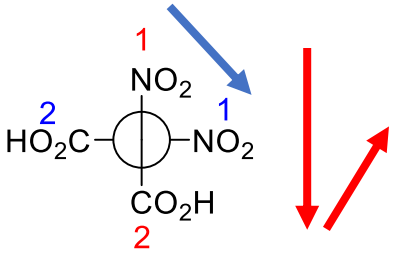

- ***CIP – S_a (counterclockwise)***
- ***Helical – P (clockwise)***

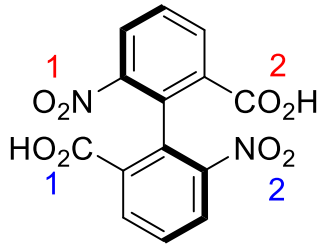

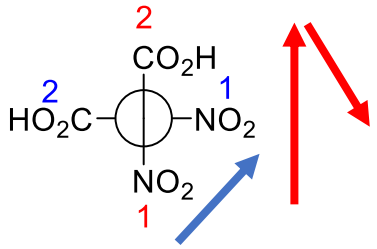

- ***CIP – R_a (clockwise)***
- ***Helical – M (counterclockwise)***

McNaught A.D., Wilkinson A. *IUPAC Gold Book.* Blackwell Scientific Publications, Oxford (**1997**)
Gustafson J. *et al. Acc. Chem. Res.* **2022**, *55*, 2904-2919;

Expanding the Definition of Atropisomers

La Plante's Expanded Definition:

Atropisomer: a subclass of conformers which arise from hindered rotation about a single bond that may or may not be isolable. These are separated into individual classes

Class 1 Example: Trifarotene

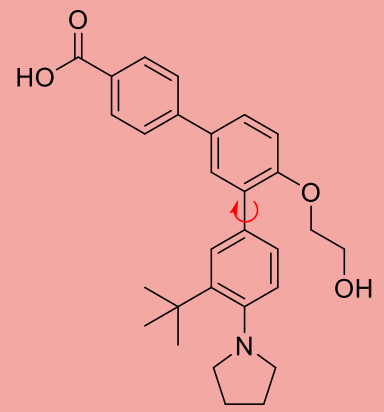

- Barrier = <20 kcal/mol
- $T_{1/2}$ = nsec to sec
- Developed as a racemate

Class 2 Example: Elagolix

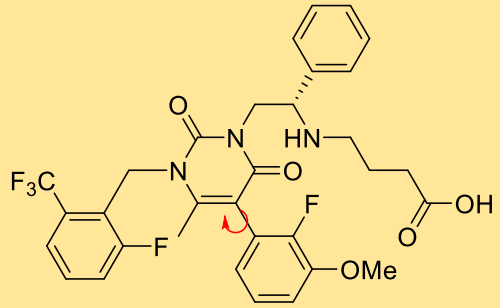

- Barrier = 20-28 kcal/mol
- $T_{1/2}$ = min to day
- Developed on a case by case basis, often as mixture

Class 3: Sotorasib

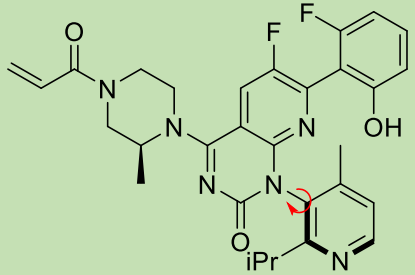

- Barrier = >28 kcal/mol
- $T_{1/2}$ = multiple months to year
- Developed as a single compound

LaPlante, S.R. *et al. J. Med Chem.* **2011**, *54*, 7005-7022
Gustafson J. *et al. Acc. Chem. Res.* **2022**, *55*, 2904-2919

The Appearance of Atropisomerism in Pharmaceuticals

Examples of Class-3 Atropisomers Recently in Clinical Trials

Esaxernone

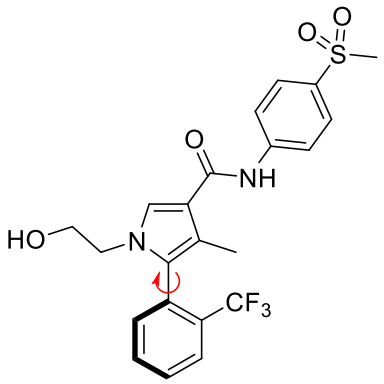

MCRA
Exelixis & Daichi-Sankyo

AZD-5991

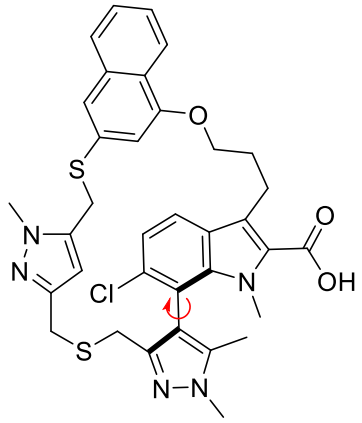

MCL-1 Inhibitor
Astrazeneca

MRTX1719

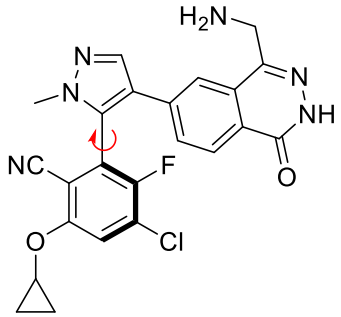

PRMT5-MTA Inhibitor
Mirati Therapeutics

BMS-986142

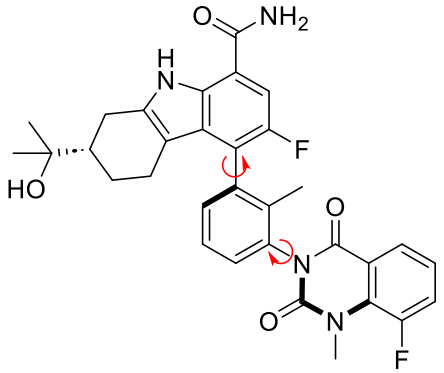

BTK Inhibitor
Bristol Myers Squibb

- There has been renewed interest in atropisomeric compounds as a mode of targeting enzymes
  - More methods to form respective atropisomers are published

- ~30% of approved drugs from 2010 to 2018 contain at least one Class-1 atropisomeric axis
  - Despite rapid interconversion of Class-1 atropisomers, drugs often can only interact in one conformation

Gustafson J. *et al. Acc. Chem. Res.* **2022**, *55*, 2904-2919
Gustafson J. *et al. Future Med. Chem.* **2018,** *10*, 409-422

Curbing Promiscuity: A Class 1 to Class 3 Perspective with Kinases

Pyrollopyrimidine-Based Kinase Inhibitors (PPYs)

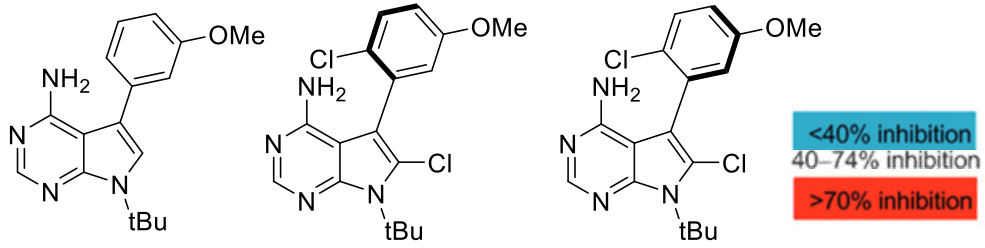

Kinase[a]	% inhibition 200 nM[b]	% inhibition 1000 nM[b]	% inhibition 1000 nM[b]	% inhibition 5000 nM[b]	% inhibition 1000 nM[b]	% inhibition 5000 nM[b]	S/R (5000 nM)[c]
Abl	37%	78%	11%	26%	36%	67%	2.57
Alk	11%	23%	6%	18%	5%	7%	0.38
Blk	38%	74%	3%	32%	21%	47%	1.46
BTK	62%	90%	10%	29%	18%	54%	1.86
CSK	36%	65%	21%	35%	19%	45%	1.28
EGFR	28%	62%	−4%	0%	10%	21%	---
Her-2	4%	16%	−2%	0%	−7%	0%	---
Fgr	69%	92%	45%	77%	58%	81%	1.05
Fyn	56%	84%	19%	44%	26%	56%	1.27
Hck	59%	80%	24%	40%	32%	50%	1.25
Kit	8%	27%	5%	26%	18%	36%	1.38
Lck	32%	79%	23%	51%	26%	54%	1.05
Lyn	58%	85%	19%	57%	36%	75%	1.31
pdgfr-a	11%	34%	3%	8%	3%	13%	1.63
pdgfr-b	6%	19%	4%	13%	13%	16%	1.23
Ret	59%	89%	35%	73%	14%	32%	0.44
Yes	63%	90%	53%	79%	53%	77%	0.97
S(40%)[c]	0.44	0.72	0.11	0.44	0.16	0.61	----

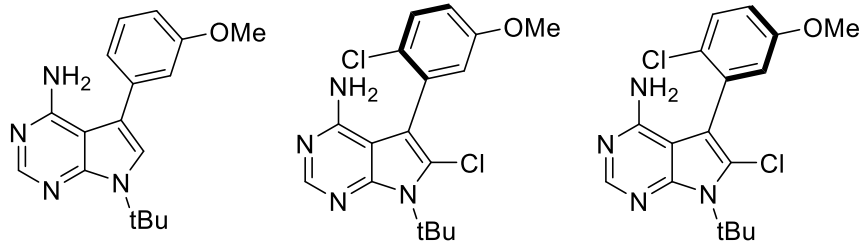

Kinase	IC_{50} **5** [nM]	IC_{50} (*R*)-**2e** [nM]	IC_{50} (*S*)-**2e** [nM]
Src	151 ± 9[b]	5570 ± 907[b]	1193 ± 170[b]
EGFR	641 ± 54[b]	>10000[c]	>10000[c]
Yes	92 ± 11[b]	895 ± 90[b]	727 ± 177[b]
Ret	128 ± 3[b]	1857 ± 482[b]	7659 ± 754[b]
Abl	244.5 ± 19[c]	>10000[c]	1432 ± 210[c]

- Rigidification leads to both less promiscuity and vastly different IC_{50} values

Gustafson J. *et al. Angew. Chem. Int. Ed.* **2015**, *54*, 11754-11759

What About Class 2 Atropisomers?

Astrazeneca's NK1 Inhibitor

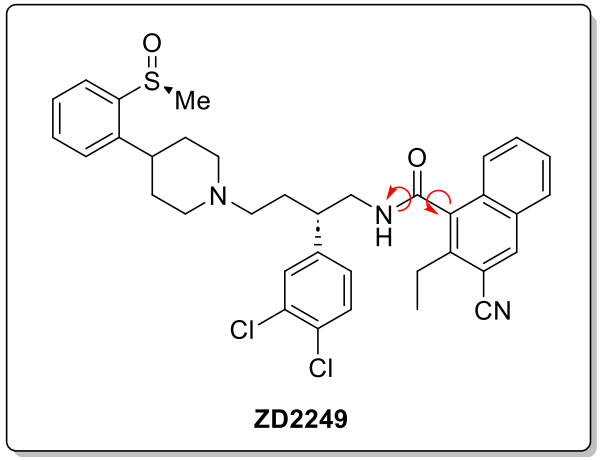

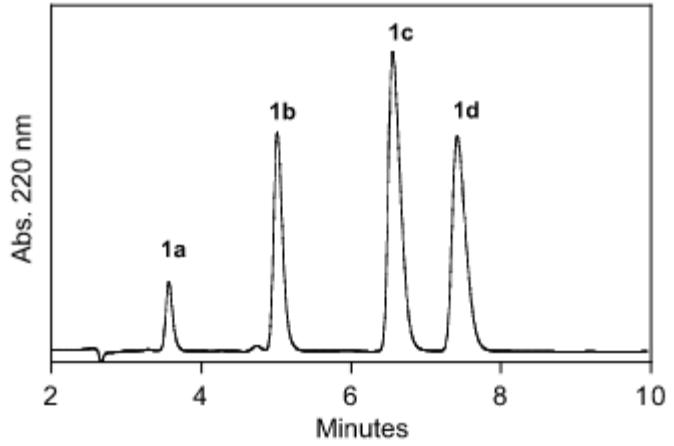

Figure 2. High pressure liquid chromatogram (HPLC) of **1** showing the resolution of the atropisomeric forms (**1a**–**1d**). Conditions: column; Phenomonex Luna C18(2) 3 µm, 4.6×75 mm; 60% methanol, 40% water (0.1% TFA), 1.5 mL/min. UV detection at 220 nM.

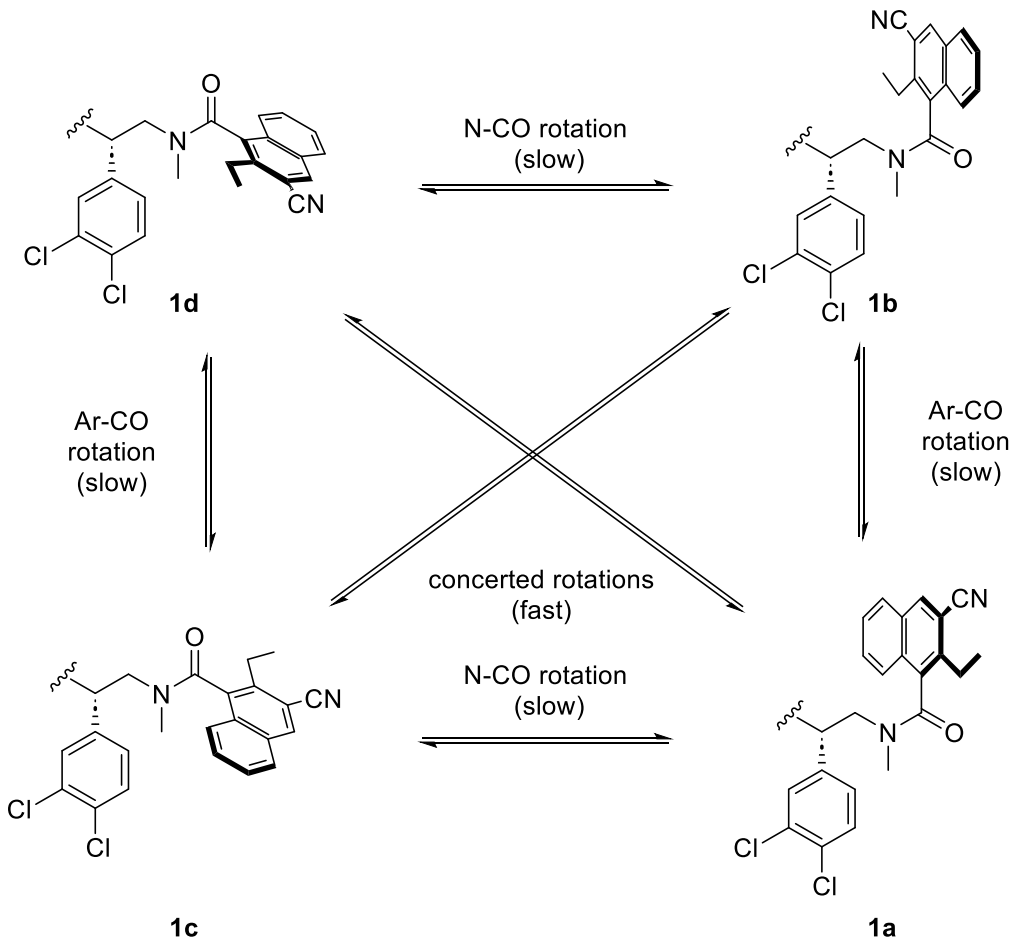

- All 4 atropisomers are visible by HPLC and NMR
- The rotational barrier half-life is 1.8 days at 37 °C
- The active atropisomer is **1d**

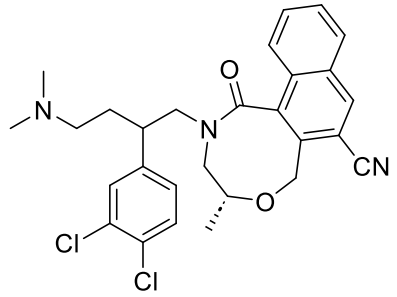

- Conversion to non-atropisomeric form maintained activity

LaPlante S. *et al. Angew. Chem. Int. Ed.* **2009**, *54*, 11754-11759
Albert J. *et al. Tetrahedron*. **2004**, *60*, 4337-4347

General Methods of Atropselective Synthesis

Chiral or Kinetic Resolution

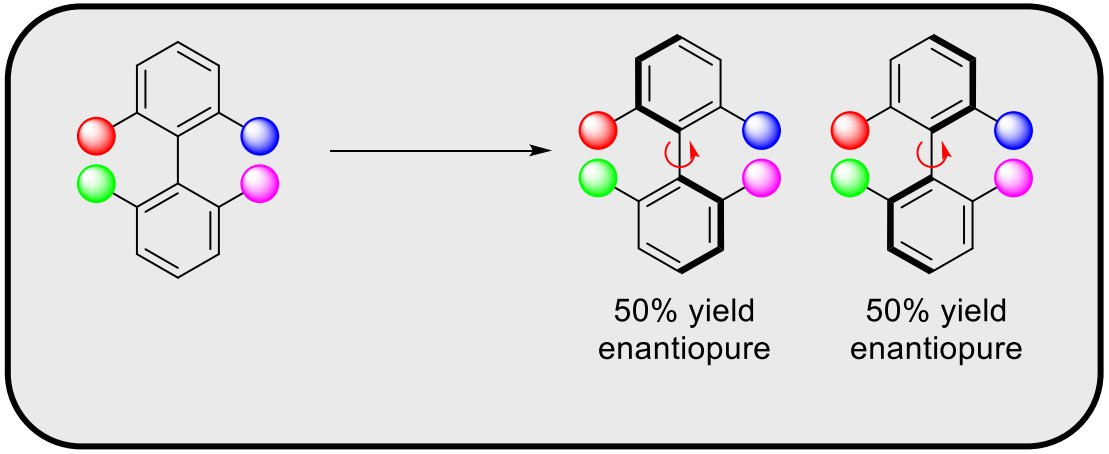

Functionalization or Dynamic Process

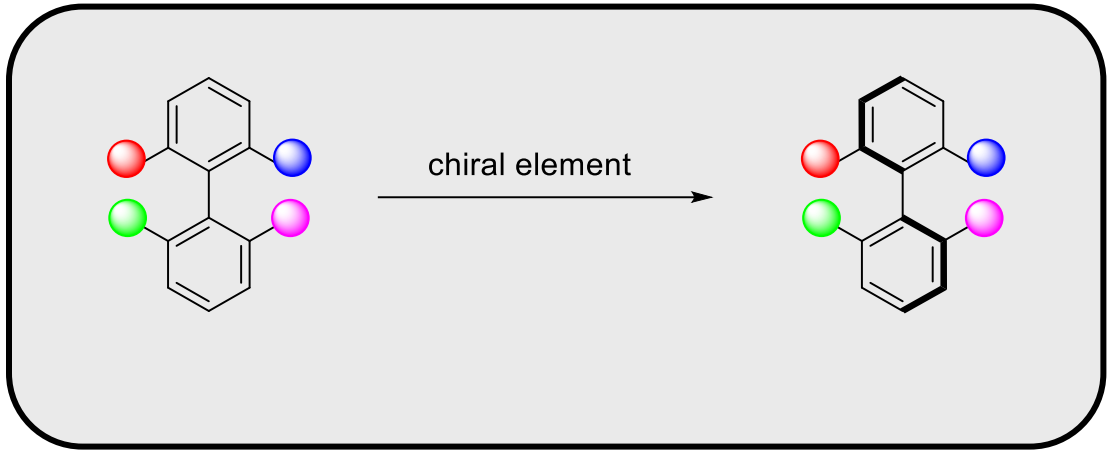

Cross Coupling

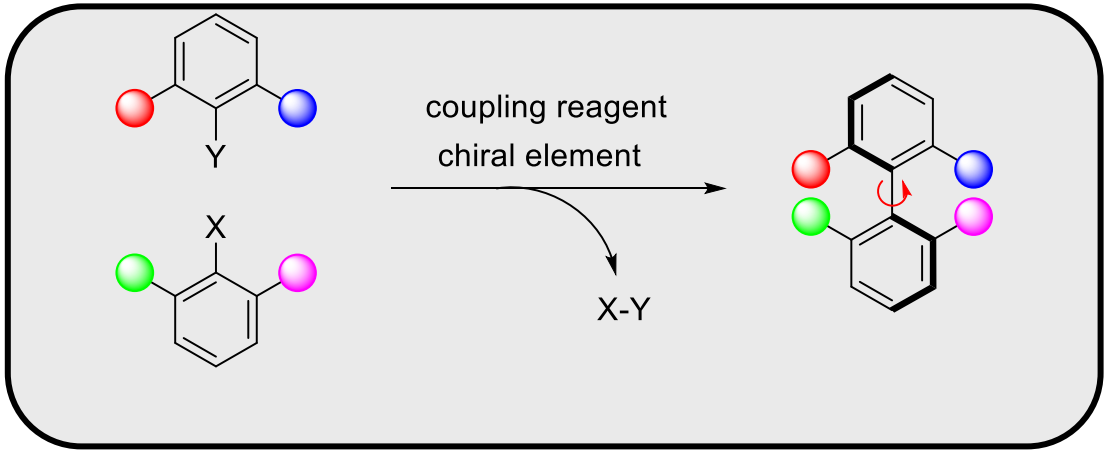

De Novo Synthesis

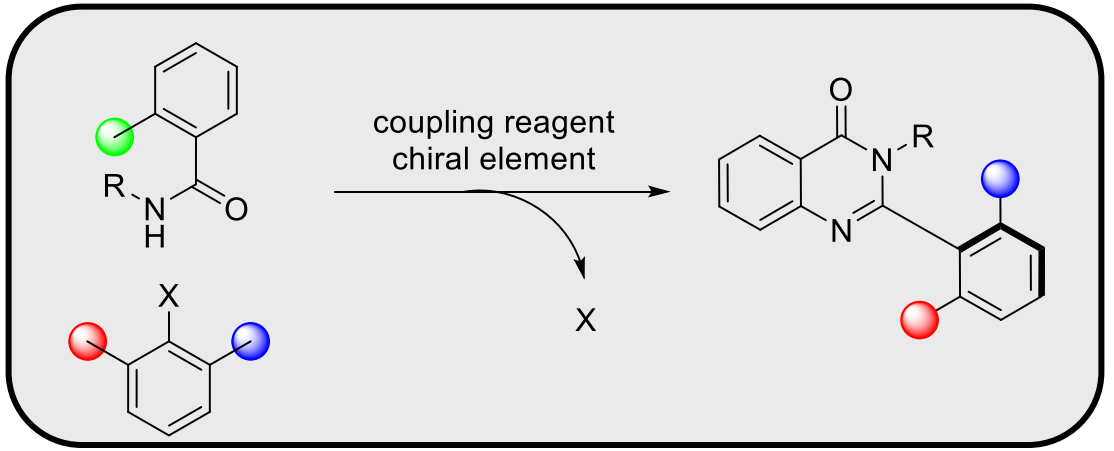

Medicinal Chemistry Resolution Case Study: PI3K Inhibitors

Class 1 Phosphoinositide 3-kinases (PI3Ks)

- Lipid kinase that catalyze phosphorylation of 3-OH of the inositol ring of phosphoinositides
  - Deregulation of PI3K activity has been implicated in cancer for PI3Kα,β,γ, and δ
- GS-9901 and other inhibitors bind in a propeller-shaped binding mode, with all three rings orthogonal
- Key Interactions:
  - Three-point interaction with Val828 and Glu826
  - Quinazolinone creates hydrophobic interactions between Trp760 and Met752
  - Pyridine is orthogonal and extends beyond ATP

Crystal Structure of PI3Kδ and GS-9901

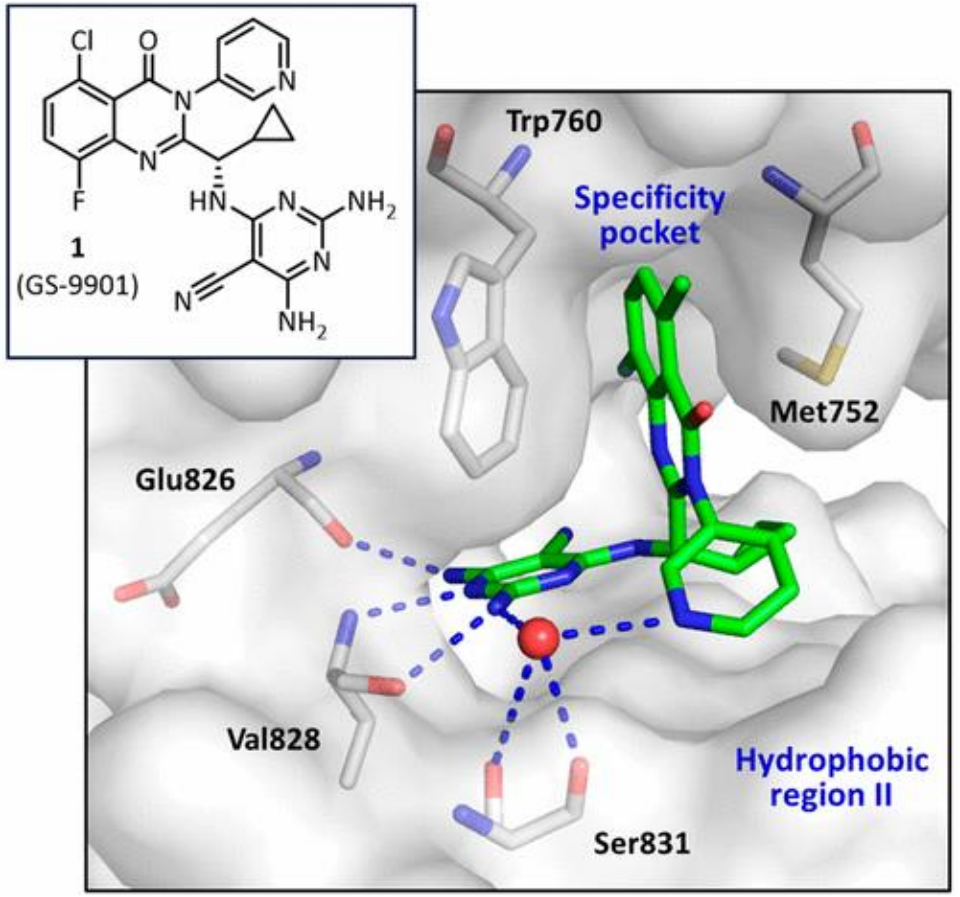

Stocks *et al. J. Med. Chem.* **2019**, 62, 10, 4815–4850
Perreault, S. *et al. Acc. Chem. Res.* **2022**, *55*, 2581-2593

Medicinal Chemistry Resolution Case Study: Inhibitor Development

Initial Discovery Route

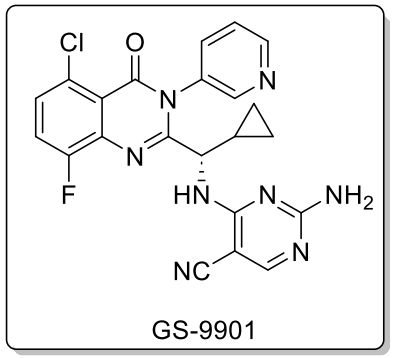

GS-9901

- Rapid acid-mediated degradation seen
  - Drug will exist in the stomach between 1-4 h at a pH of 1.5-3.5

PI3K Inhibitor Selectivity and Stability

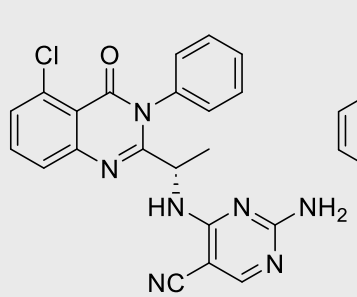

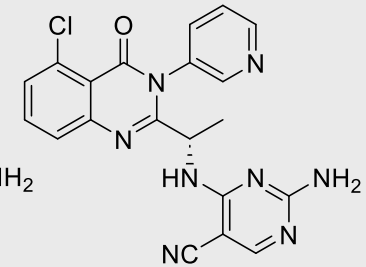

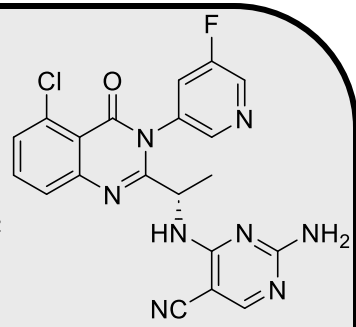

	First Generation	Second Generation	Third Generation
PI3Kδ IC_{50} (nM)	0.1	0.6	1.7
PI3Kβ IC_{50} (nM)	9.4	100	741
β / δ selectivity	94x	166x	435x
$t_{90}/_{50}$ [pH 2, 40 C] (h)	ND / 358	0.2 / 2.7	0.5 / 3.6

Patel L. *et al. J. Med Chem.* **2016**, *59*, 9228-9242
Patel L. *et al. Acc. Chem. Res.* **2022,** *55*, 2581-2593

Medicinal Chemistry Resolution Case Study: Modifying Chemical Stability

Proposed Mechanism of Acid-Mediated Degradation

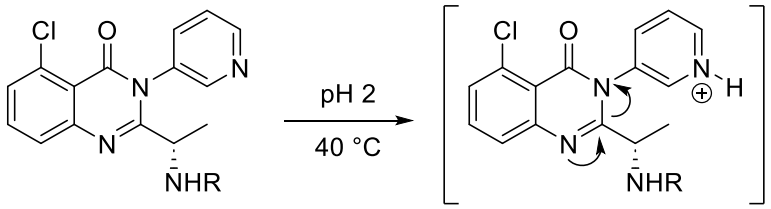

- Estimated pKa of pyridine:
  - Unsubstituted = 4.3
  - 3-fluoro = 1.9
- Disfavoring coplanarity may decrease pKa further

Resolution of Diastereomers

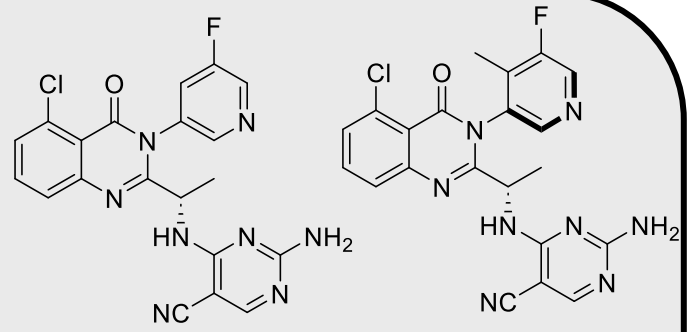

	Third Generation	Fourth Generation
PI3Kδ IC_{50} (nM)	1.7	0.3
PI3Kβ IC_{50} (nM)	741	120
β / δ selectivity	435x	400x
$t_{90}/_{50}$ [pH 2, 40 C] (h)	0.5 / 3.6	4.6 / 30

Patel L. *et al. J. Med Chem.* **2016**, *59*, 9228-9242
Patel L. *et al. Acc. Chem. Res.* **2022,** *55*, 2581-2593

Process Resolution Case Study: Sotorasib and KRAS^{G12C} Inhibition

KRAS^{G12C} the "Undruggable" Target

- Kirsten rat sarcoma (KRAS) gene is an essential mediator of intracellular signaling pathways
  - KRAS protein is a GTPase converting GTP to GDP
  - KRAS^{G12} mutations account for 89% of KRAS cancers with G12C accounting for 14% of these
- Considered undruggable for over 30 years:
  - Picomolar affinity to GDP/GTP
  - Lack of hydrophobic pockets, preventing efforts towards allosteric inhibitors
- Sotorasib (AMG 510) contains a Class-3 and Class-2 atropisomeric axis

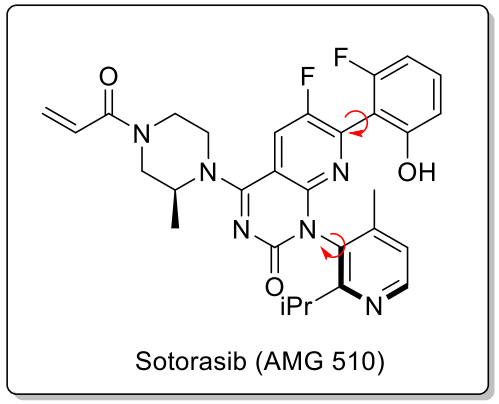

Sotorasib (AMG 510)

Crystal Structure of Sotorasib with KRAS

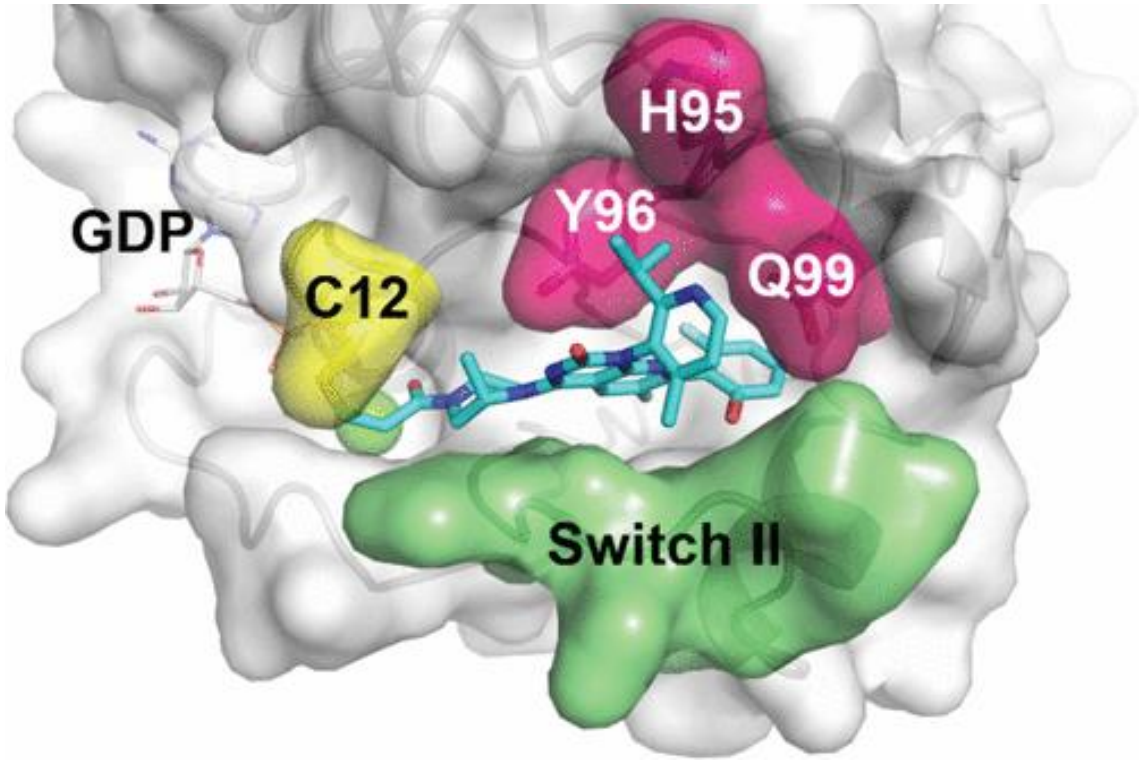

- Key Interactions:
  - Acrylamide forms covalent bond with Cys12
  - Quinazolinone core occupies the Switch II pocket
  - Isopropyl fills pocket created by His95, Tyr96, Gln99

Lanman *et al. J. Med. Chem.* **2020**, *63*, 1, 52–65; Canon *et al. Nature*. **2019**, *575*, 217-223;
Tang *et al. Cancer Gene Ther.* **2022**, *29*, 875-878;

Process Resolution Case Study: Designing a Route

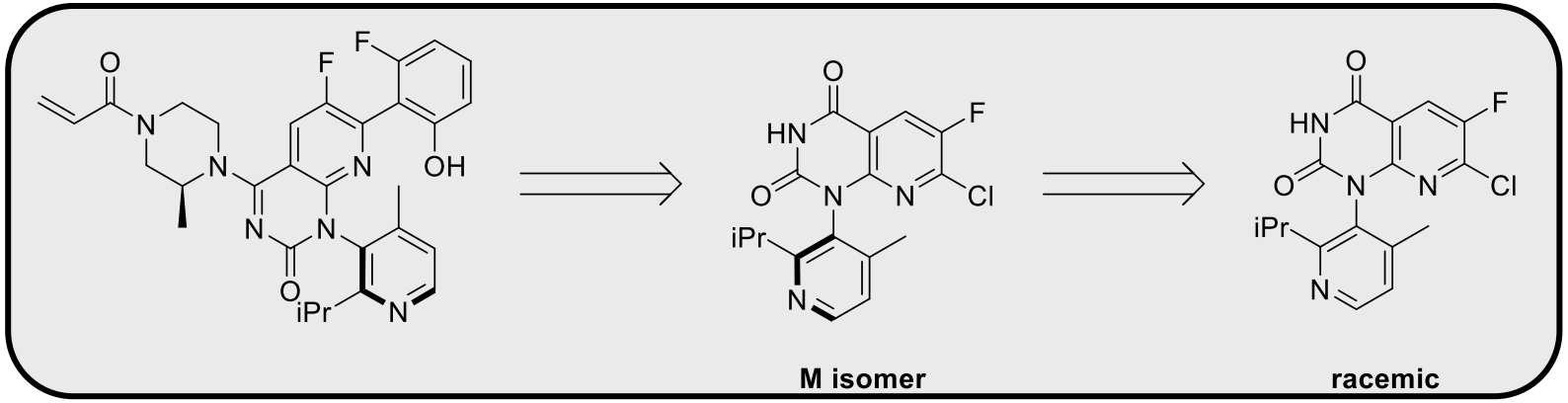

"Given an aggressive timeline to deliver kilogram quantities of ***M*,** it was determined that chromatographic separation of the racemate would be pragmatic"

- The targeted enantiomeric ratio of **M:P** was at least 99.7:0.3 for asymmetric catalysis
- Preparative chromatography was unsustainable for commercialization

Lanman *et al. Acc. Chem. Res.* **2022**, *55*, 2892-2903;
Parsons *et al. Org. Process. Dev.* **2022**, *26,* 2629-2635

Process Resolution Case Study: Commercial Route to Sotorasib

Lanman *et al. Acc. Chem. Res.* **2022**, *55*, 2892-2903; Parsons *et al*. WO 2021097212 A1, **2021**
Parsons *et al. Org. Process. Dev.* **2022**, *26,* 2629-2635

Process Resolution Case Study: Crystallization

Initial Crystallization Screening

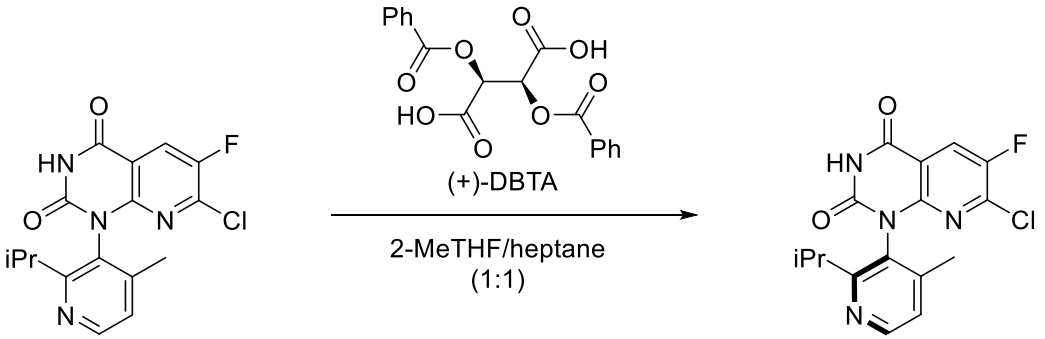

initial result 81:19 (M:P)

	M/P ratio in solids (*M/P* ratio in the supernatant)			
2-MeTHF/heptane 12L/g (vol/vol)	2 eq (+)-DBTA	1.5 eq (+)-DBTA	0.67 eq of (+)-DBTA	0.5 eq of (+)-DBTA
8:1	93:7 (29:71)	90:10 (29:71)	87.5:12.5 (33:67)	72:28 (38.5:62.5)
4:1	90:10 (23:77)	86:14 (23:77)	86:14 (29:71)	85:15 (29:71)
2:1	86:14 (17:83)	85:15 (17:83)	82:18 (17:83)	84:16 (17:83)

- By charging heptane and a seed after (+)-DBTA and the racemate were dissolved resulted in >99.9:0.1 *M/P* ratio of a ***M*** cocrystal solvate (42%/ 50% theoretical yield)

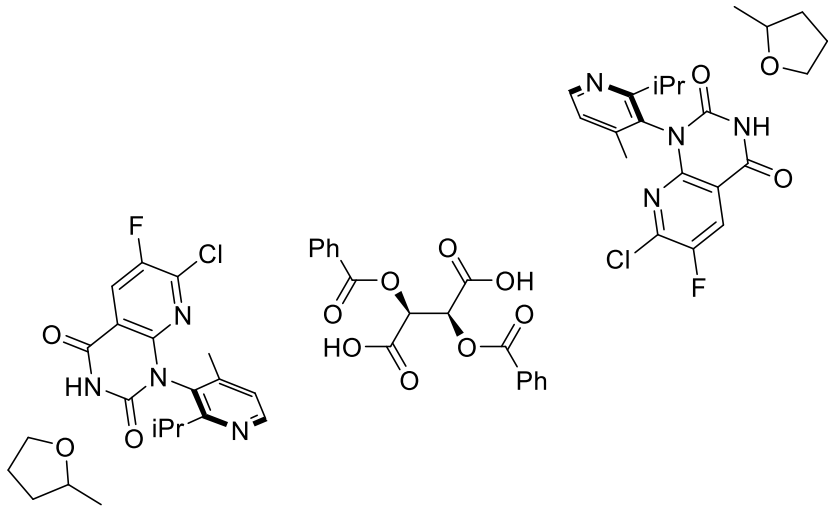

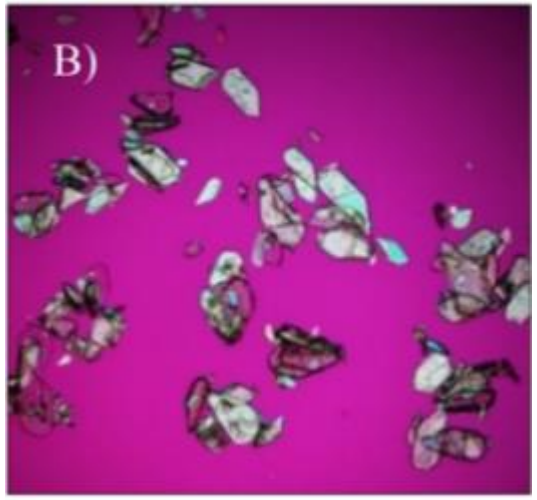

Parsons *et al. Org. Process. Dev.* **2022**, *26,* 2629-2635;

Crystallization Dependence on Concentration of (+)-DBTA

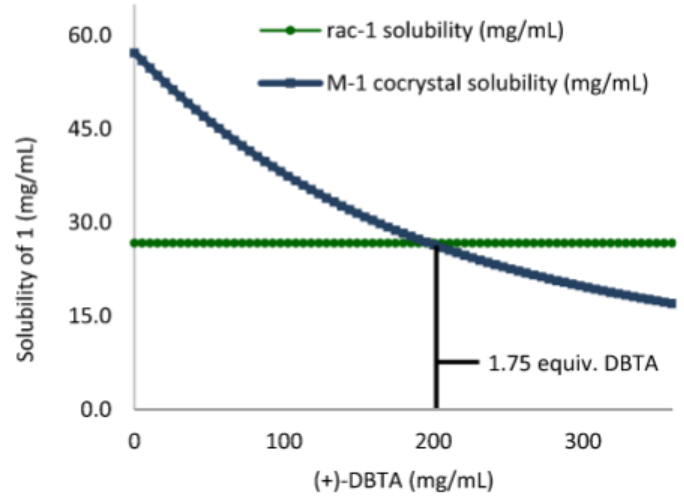

Figure 2. Solubility of *rac*-**1** and *M*-**1** in 2-MeTHF/heptane (7:2) at 65 °C (seeding conditions) as a function of [DBTA].

Process Resolution Case Study: Recycling the *P* Atropisomer

Final Crystallization of *M* Atropisomer

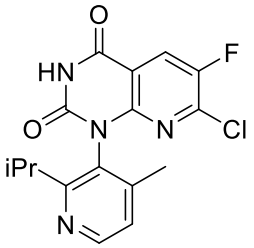

1. (+)-DBTA (3 eq), 2-MeTHF (8 L/kg), 75°C
2. Heptane (1 L/kg), 45°C
3. ***M*** cocrystal seed (0.1 wt%)
4. Cool to 20 °C
5. Heptane (4 L/kg)
6. Isolate by filtration
7. Wash 1:1 v/v 2-MeTHF/heptane

→ **M cocrystal solvate**
42% yield, >2000:1 M/P
\+
supernatant

Racemization Conditions

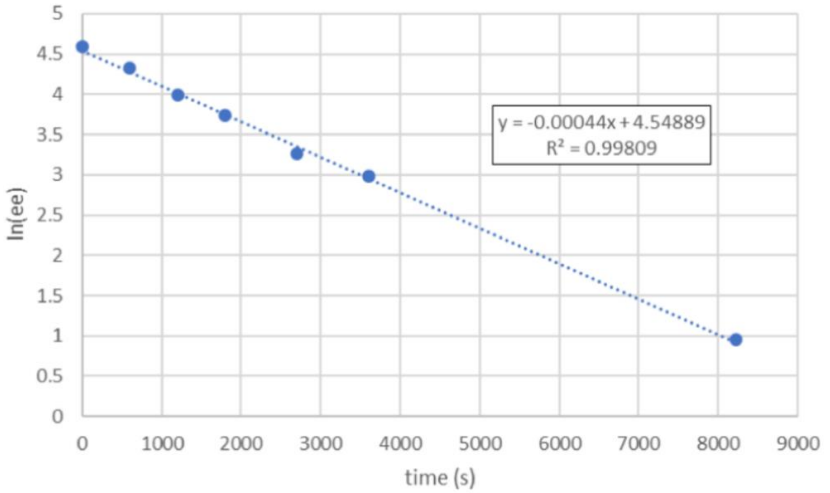

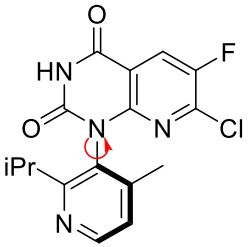

P

DPE, 280 °C

- $T_{1/2}$ = 26.2 min
- ΔG_{rot} = 42.3 kcal/mol

Direct racemization of supernatant was impractical due to high boiling solvents and 2.75 eq excess of (+)-DTBA

Avoiding Precipitation of (+)-DBTA Salts

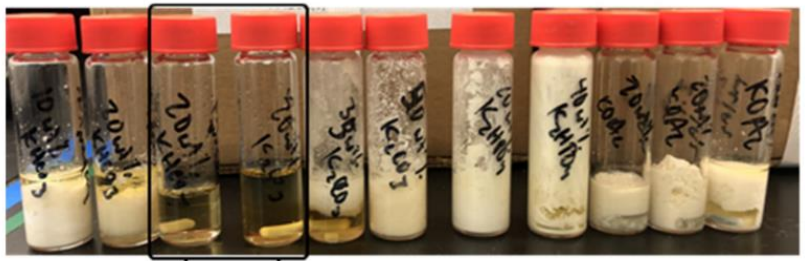

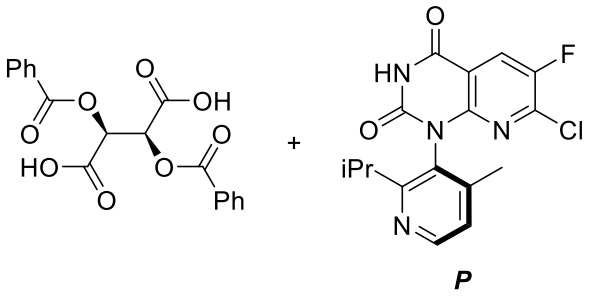

P

in 8:5 2-MeTHF/heptane (13 vol)

1. 20 wt% aq K_2CO_3 (2:1 v/v ML/Aq)
2. Charge ML
3. Separate Layers

→

4. Wash with water
5. Distill to 2 L/kg
6. Charge heptane (2 L/kg)
7. Filter and Dry

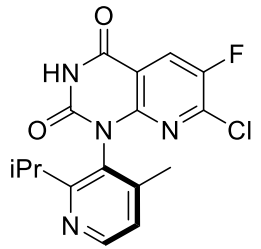

P

90% yield, 88:12 *(P:M)*
crystalline solid

Beaver *et al. Org. Process. Dev.* **2022**, *26,* 2636-2645

Process Chemistry Resolution Case Study: Design of a Plug-Flow Reactor

Considerations in Reactor/Reaction Design

- Heat transfer
  - Kinetic model suggested temperatures more than 300 °C would be required

- Solvent Choice
  - Solvent affects purity profile of process with high ***P*** and low **racemate** solubility desired
  - Preliminary crystallization of the **racemate** upon could clog lines

- Thermal mass
  - The ability of a reactor can absorb and store heat can widely change the process
  - In their initial demonstration, this was at a factor of 33, compared to 2 in a standard glass reactor due to the jacket-side heat transfer fluid

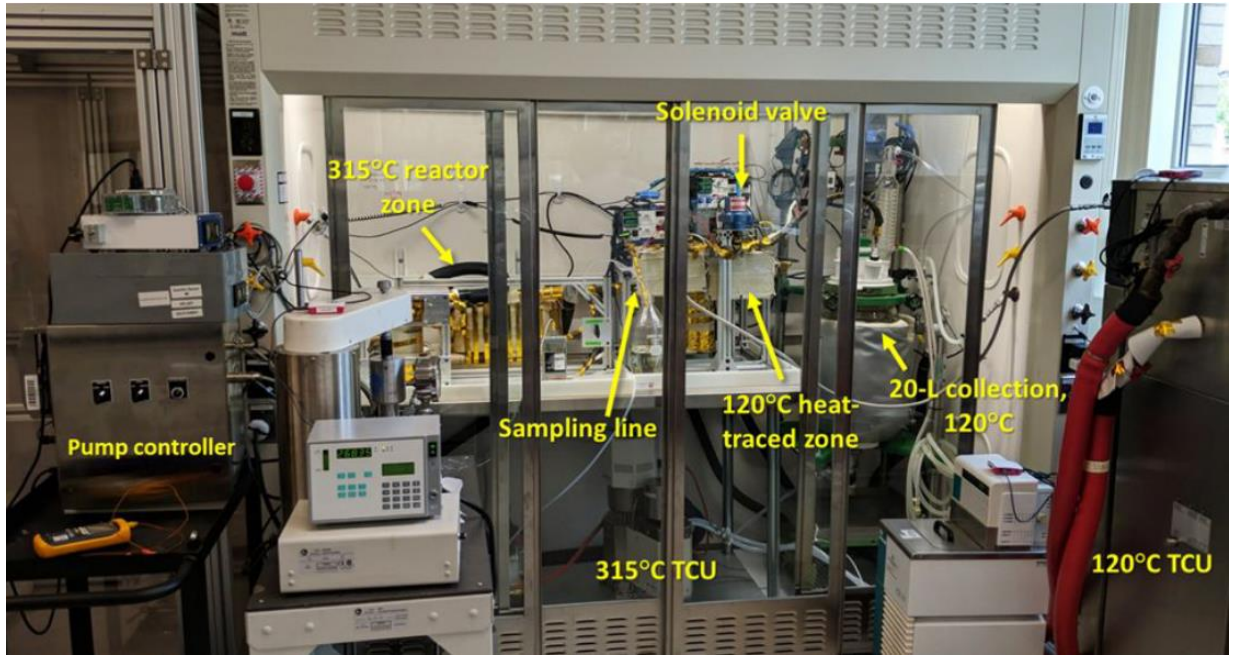

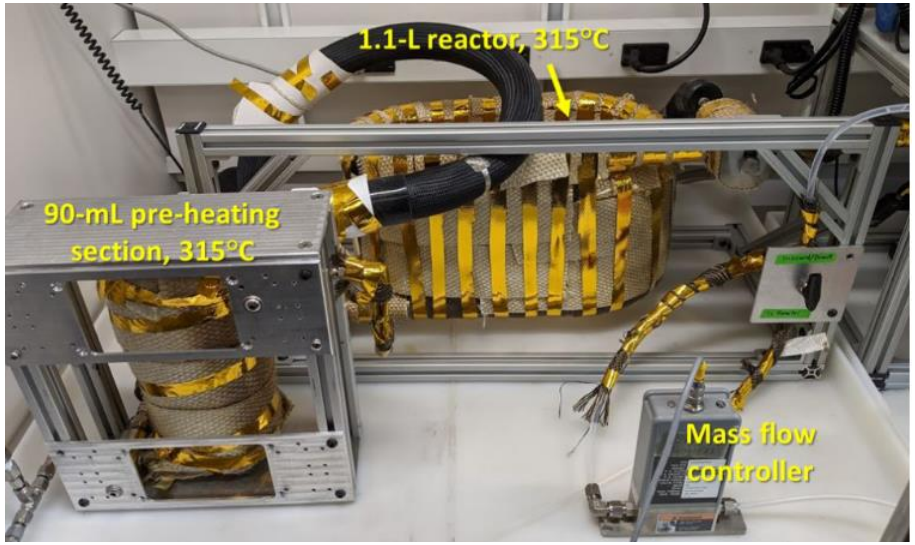

Beaver *et al. Org. Process. Dev.* **2022**, *26,* 2636-2645

Process Chemistry Resolution Case Study: Design of a Plug-Flow Reactor

Considerations in Reactor/Reaction Design

- Heat transfer
  - Kinetic model suggested t
    than 300 °C would be rec
- Solvent Choice
  - Solvent affects purity pro
    high ***P*** and low **racemat**
  - Preliminary crystallizatio
    upon could clog lines
- Thermal mass
  - The ability of a reactor ca
    heat can widely change th
  - In their initial demonstration, this was at a factor of 33, compared to 2 in a standard glass reactor due to the jacket-side heat transfer fluid

Final Result:

- Recrystallization in anisole at 0 °C afforded the racemic product in 77% yield (50.5:49.5 *P:M)* as a crystalline solid
- Only 2% yield loss associated with decomposition of **P** isomer
- 20% of remaining mass balance associated with losses to crystallization
- PMI reduced by 58%

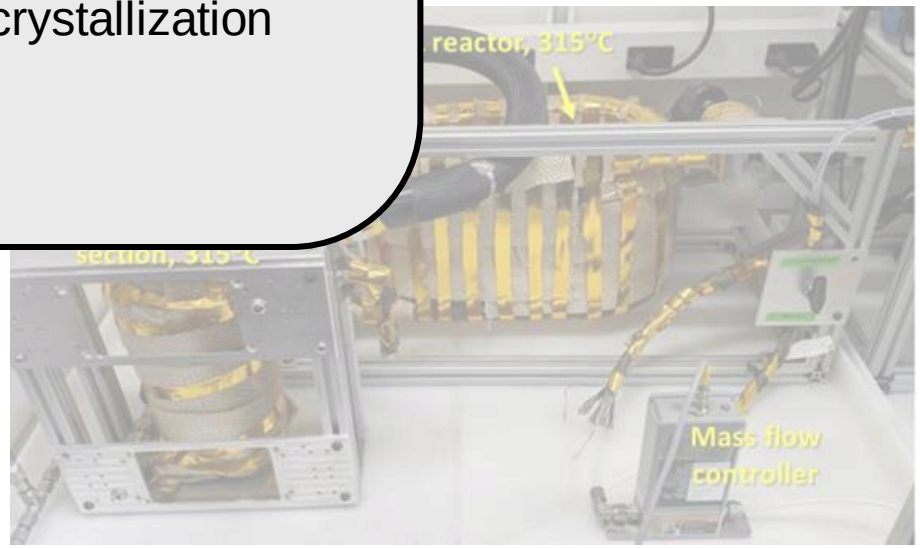

Beaver *et al. Org. Process. Dev.* **2022**, *26,* 2636-2645

Cross-Coupling Case Study: GDC-6036 and KRAS^{G12C} Inhibition

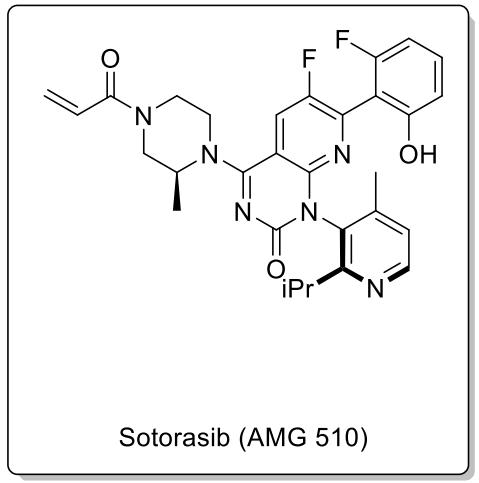

Sotorasib (AMG 510)

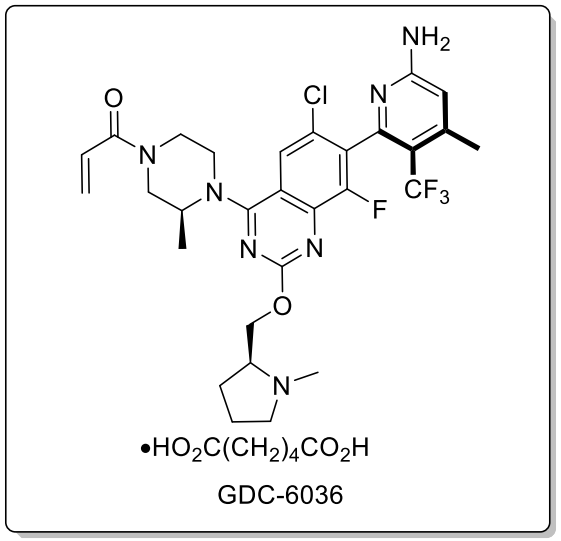

GDC-6036

	KRAS G12C HRTF IC_{50} (nM)	KRAS G12C k_{inact}/K_i $(M*s)^{-1}$	Median Cell Prolif IC50 (nM) / Selectivity
GDC-6036	0.0029	710,000	0.18 / 16,000 X
Sotorasib	1.4	7,900	3.4 / >1800 X
Comparison	482x	90x	25x

GDC-6036 is significantly more potent

Crystal Structure of GDC-6036 with KRAS^{G12C}

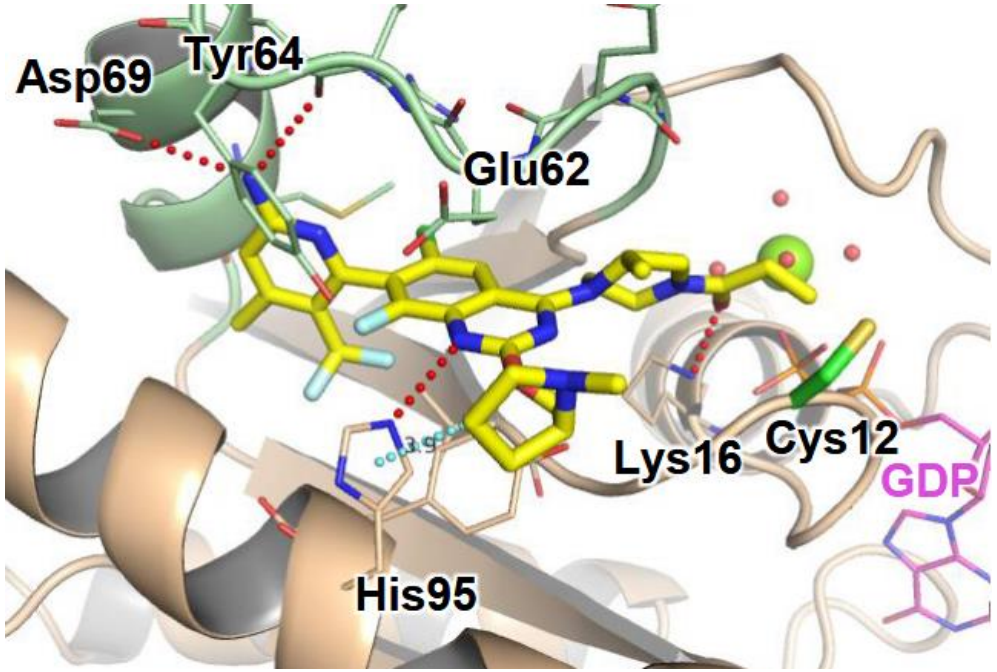

- Key Interactions:
  - Same key interactions of acrylamide and quinazolinone
  - Pyrrolidine interacts with Lys16
  - The aminopyridine interacts with Asp69, Tyr64

Purkey, H. *Discovery of GDC-6036, a clinical stage treatment for KRAS G12C-positive cancers.* **11 April 2022** AACR National Meeting, New Orleans

Cross-Coupling Case Study: Scouting GDC-6036 Synthesis

Retrosynthetic Plan

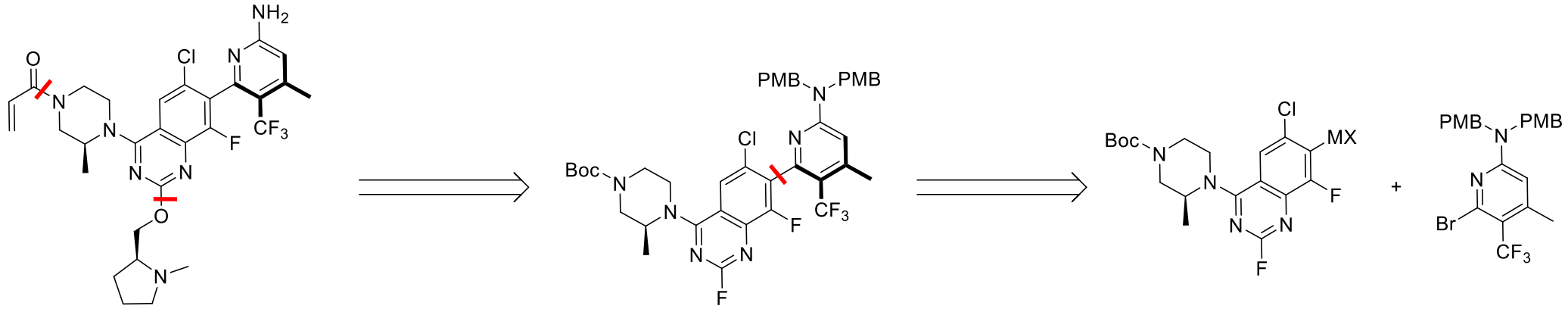

Initial Hit with Negishi Cross Coupling

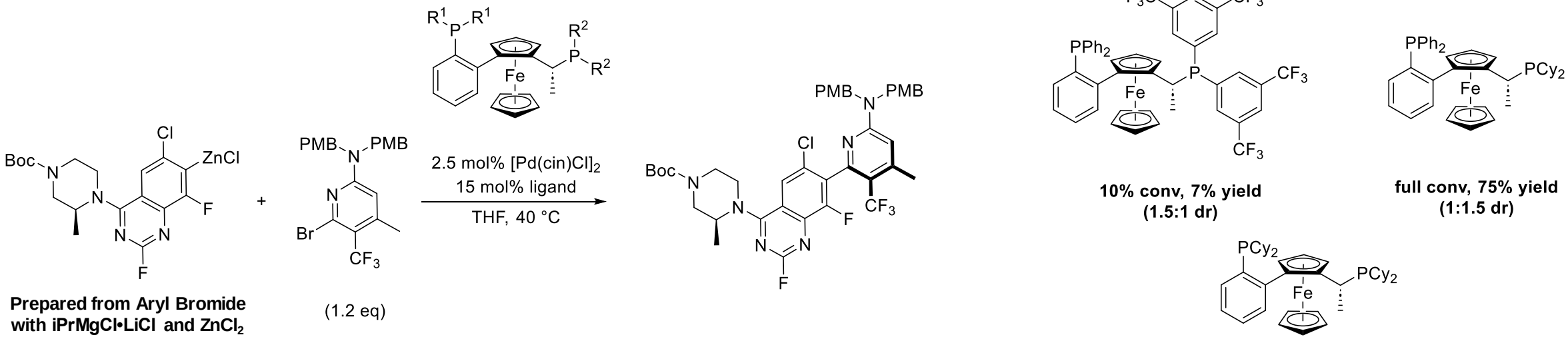

Xu *et al. J. Am. Chem. Soc.* **2022**, 144, 20955-20965

Cross-Coupling Case Study: A Chemoinformatic Approach

Defining a Workflow for finding an Optimal Ligand

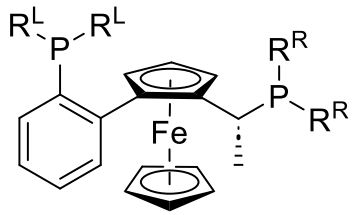

11 commercial Walphos ligands were used to define a training set

Featurized with bond lengths, angles, %V_{bur}, NBO charges, bond energies

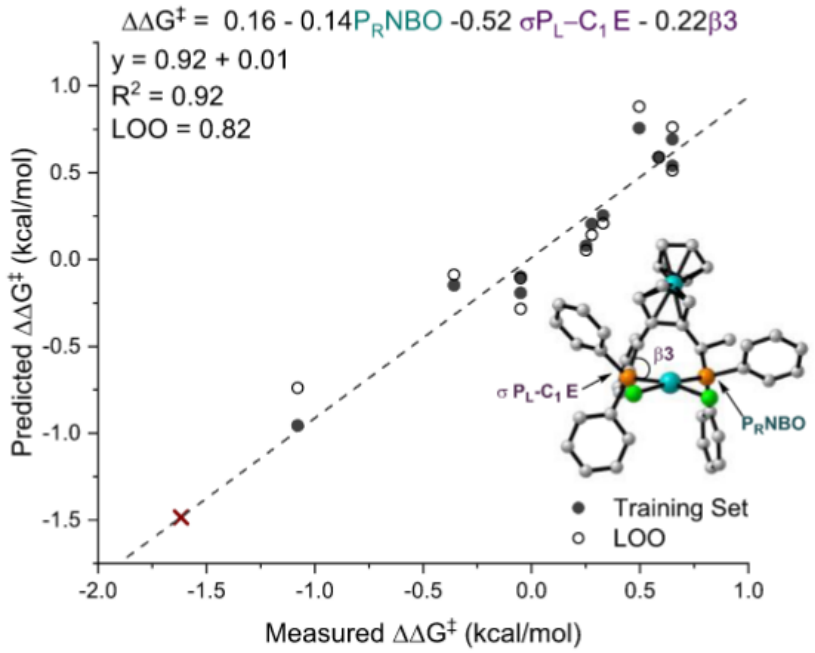

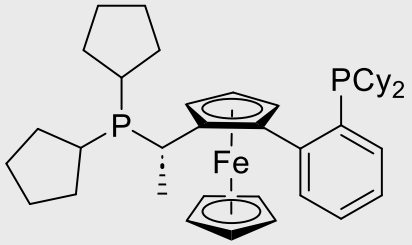

isolated : 67% yield (98:2 dr)
in situ: 85% yield (92:8 dr)

- ❖ Successfully provided a route towards synthesis of GDC-6306
- ❖ This ligand was only successful for the original coupling
- ❖ Execution of this workflow to other hetero-biaryl couplings provided similar results

- ❖ Features were extracted and regressed with a forward stepwise linear regression
- ❖ Additional Walphos analogues were virtually screened and prioritized based on structure similarity and accessibility

Xu *et al. J. Am. Chem. Soc.* **2022**, 144, 20955-20965

Cross-Coupling Case Study: Scaling the Reaction

Second Generation Atropselective Negishi

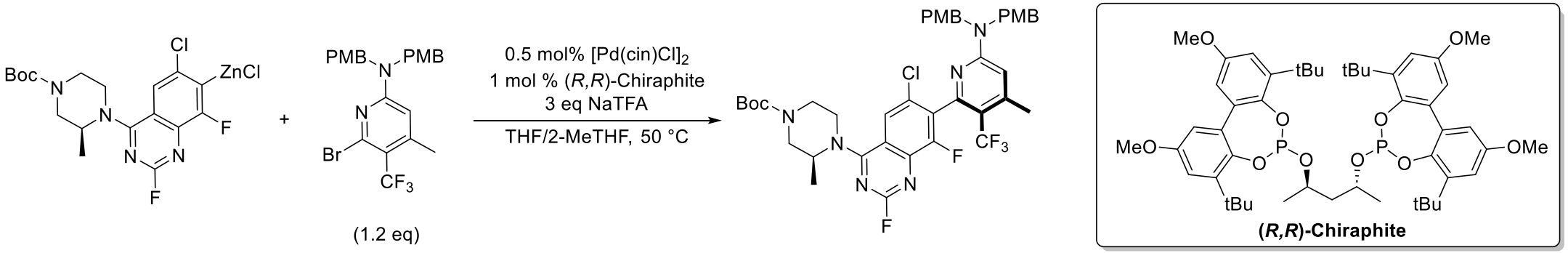

- Walphos abandoned due to high catalyst and ligand loadings, along with synthetic challenges at scale
- NaTFA helps is believed to sequester large amounts of chloride ions to help push conversion

Quinazoline Organomagnesium Instability Above Cryogenic Temperatures

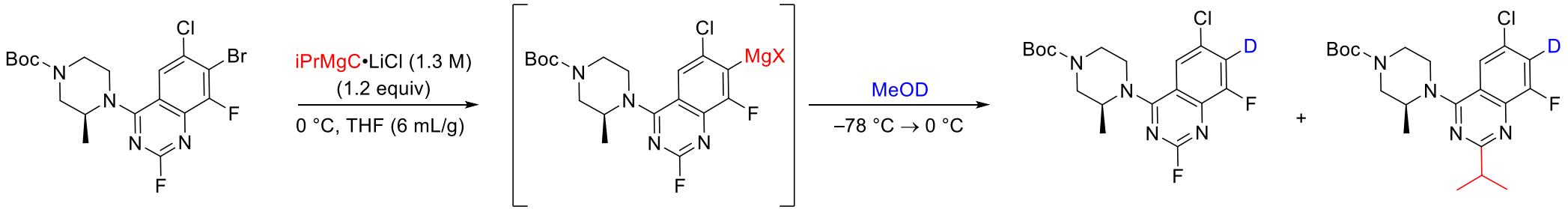

- Competitive S_NAr at the quinazoline plagued scaling efforts

Aging Time	Desired Product % wt Assay	S_NAr Product % wt Assay
1	94	1.1
5	87	3.6
15	79	10

Xu *et al. Org. Lett.* **2022**, 144, 20955-20965; Kelly S. *et al.* **2023** ASAP Article, doi.org/10.1021/acs.oprd.3c00164

Cross-Coupling Case Study: Scaling the Reaction

ReactIR Monitoring of Reaction

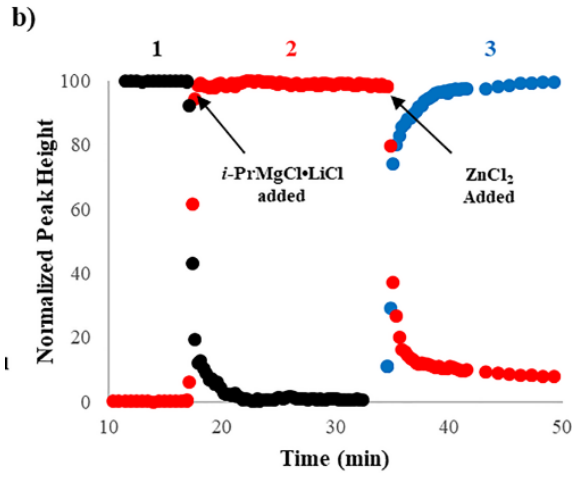

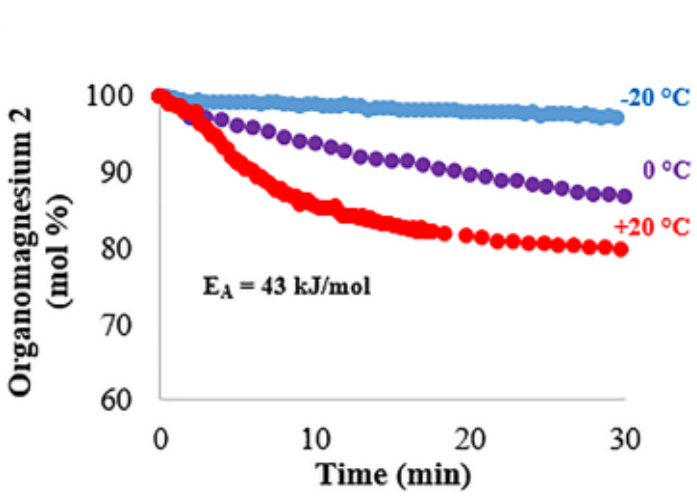

Predicted Performance

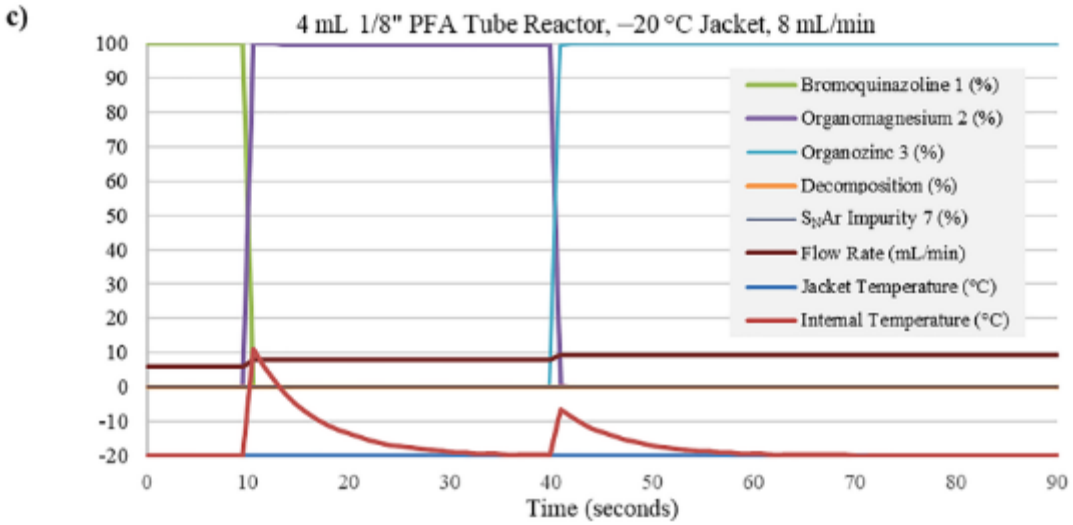

- Near instantaneous Br-Mg exchange at -20 °C
  - No accumulation of *i*PrMgCl•LiCl suggests efficient mass transfer would have a larger impact on reaction rate
- Calorimetry studies showed Br-Mg exchange enthalpy of -172 kJ/mol (25 °C) while Mg-Zn transmetalation is -88 kJ/mol (12 °C)
  - This adiabatic rise in temperature means heat transfer is essential within the reactor
- Performance for a Plug Flow Reactor (PFR) was predicted, showing that with a -20 °C jacket, both decomposition and S_NAr impurities would be lost
- A continuous flow proof-of-concept was created and then piloting campaign was created running on 3.5 kg scale (7.33 mol)
  - 72.1% yield, 98.9% HPLC purity, 98.4:1.6 dr

Kelly S. *et al.* **2023** ASAP Article. doi.org/10.1021/acs.oprd.3c00164

Chirality Transfer in De Novo Synthesis : BMS-986142 and BTK Inhibition

Designing a BTK Inhibitor

- Bruton's Tyrosine Kinase (BTK) is nonreceptor tyrosine kinase which is essential for B cell receptor activation and proliferation
  - Mutation of BTK can result in developmental defects in B cells
  - Inhibition of BTK has been shown to be an effective strategy for treating lupus and rheumatoid arthritis

- BMS-986142 contains two different atropisomeric axis
  - Removal of atropisomeric axis reduced bioactivity

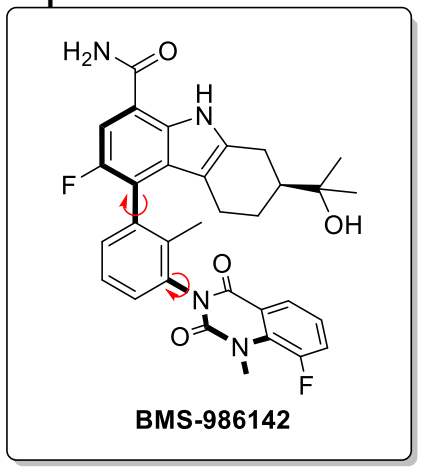

BMS-986142

Crystal Structure of Sotorasib with KRAS

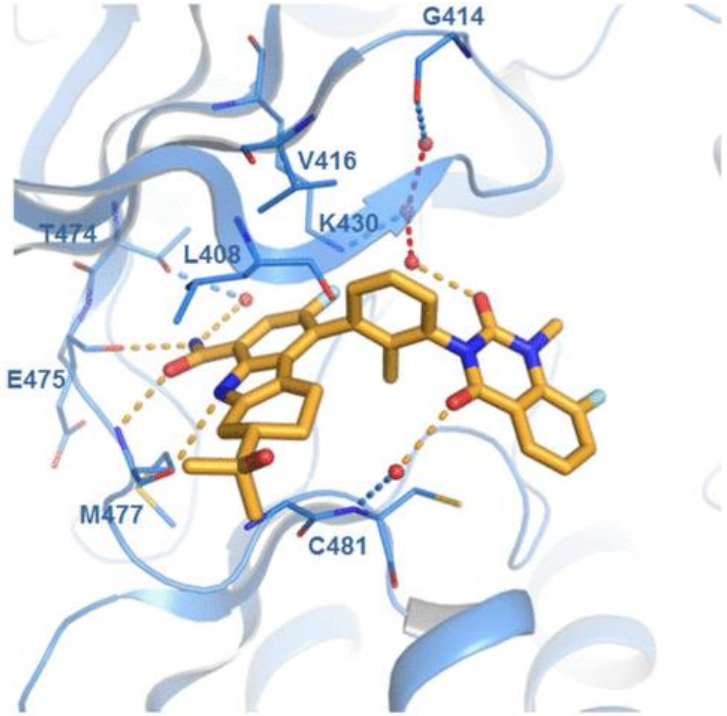

1.5 Å structure

- Key Interactions:
  - Tetrahydrocarbazole and carboxamide have hydrogen bonding with Met477
  - The quinazoline dione is engaged in hydrogen bonding network with water to Cys481, Lys430, Gly414

Watterson *et al. J. Med. Chem.* **2016**, 59, 19, 9173–9200

Chirality Transfer in De Novo Synthesis: Initial Medicinal Chemistry Route

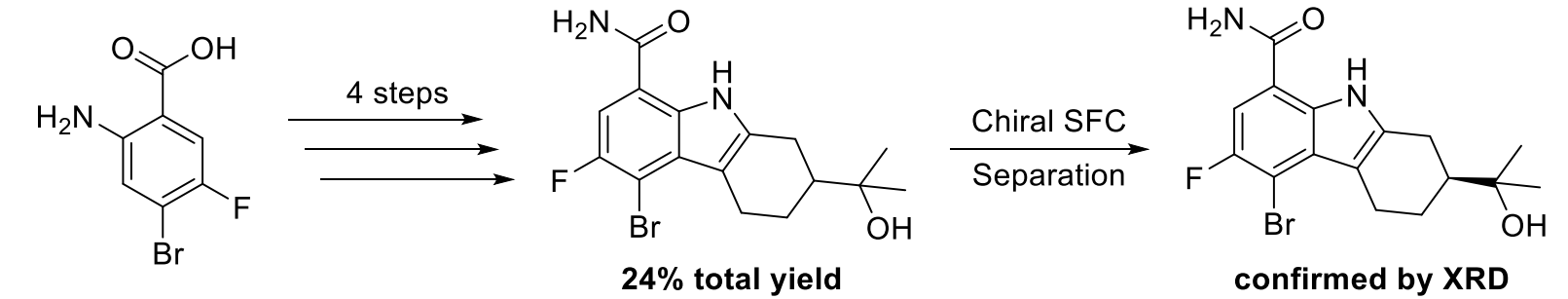

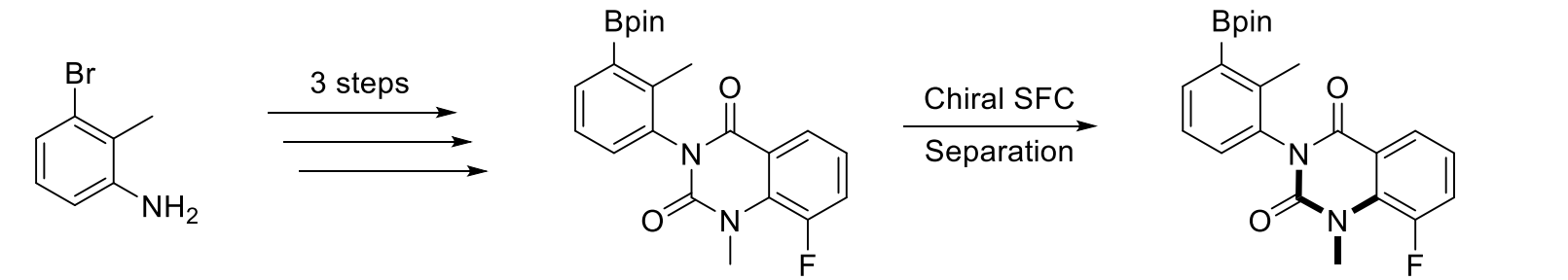

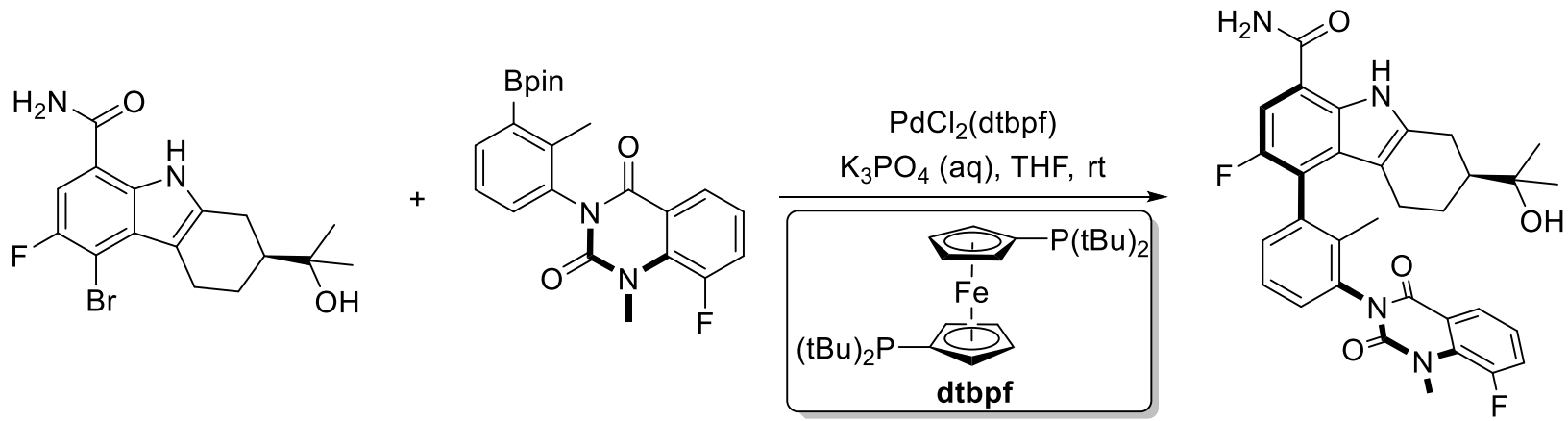

Involved 3 separate chiral SFC runs

Watterson *et al. J. Med. Chem.* **2016**, 59, 19, 9173–9200;

Chirality Transfer in De Novo Synthesis: Designing an Optimal Route

1. Late stage carbazole construction

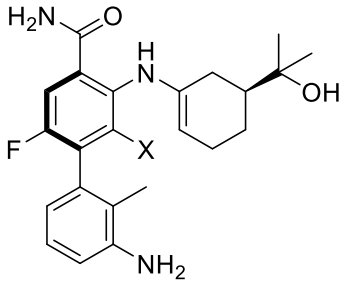

X = Br, Cl, OTs, OMs

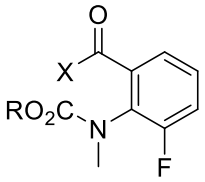

X = OH, O
R = Alkyl, Ph

Auxilary CC

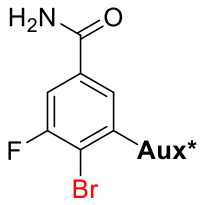

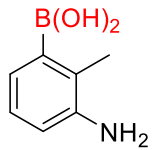

Asymmetric Heck

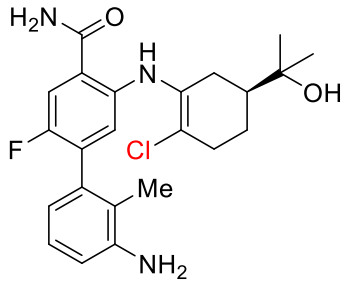

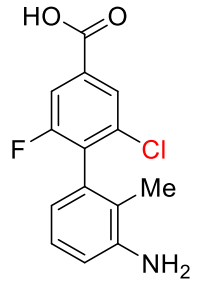

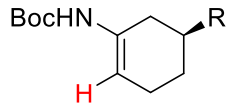

Abandoned early on due to expense and challenging substrates

2. Optimize Existing Cross Coupling

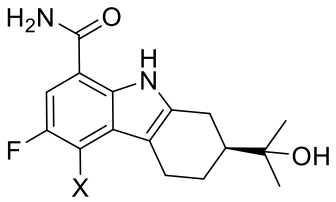

X = Br, Cl, OTs, OMs

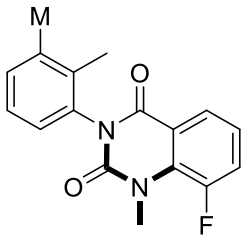

M = BY_2, BF_3K, MgCl, ZnCl

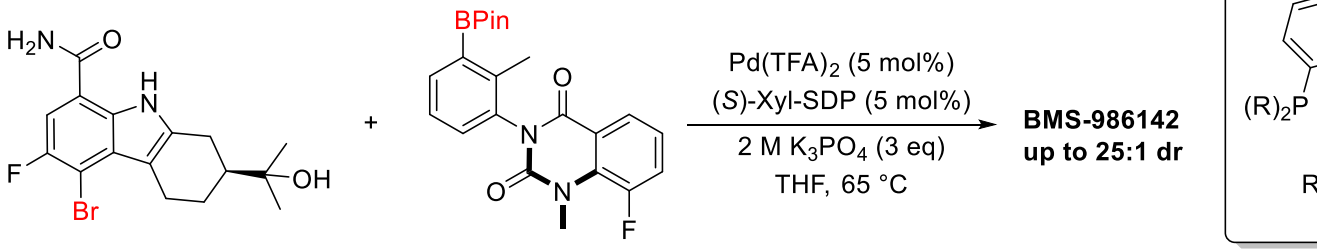

Chiral chromatography of boronic ester necessitated new process route

3. Late Stage Construction of C-N axis

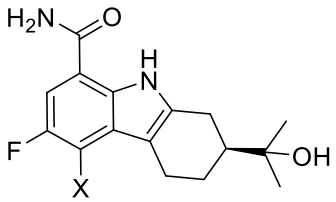

X = Br, Cl, OTs, OMs

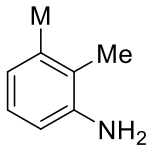

M = BY_2, BF_3K, MgCl, ZnCl

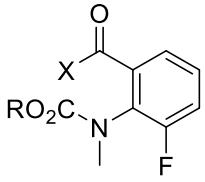

X = OH, O
R = Alkyl, Ph

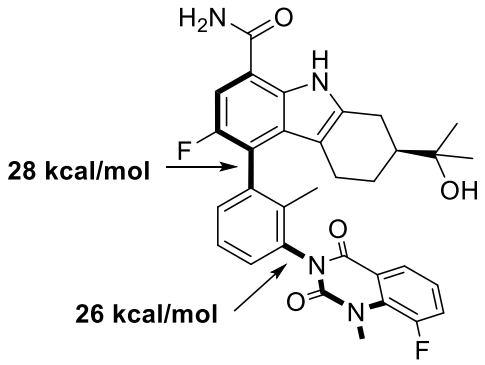

Construction of C-C axis could be used to enforce C-N axis construction

Watterson *et al. J. Med. Chem.* **2016**, 59, 19, 9173–9200;
Watterson, S. *et al. ACS Symposium Series*, Vol 1423, **2022**

Chirality Transfer in De Novo Synthesis: Designing an Optimal Route

Choosing a Ligand for Scale-Up of the Suzuki-Miyaura Coupling

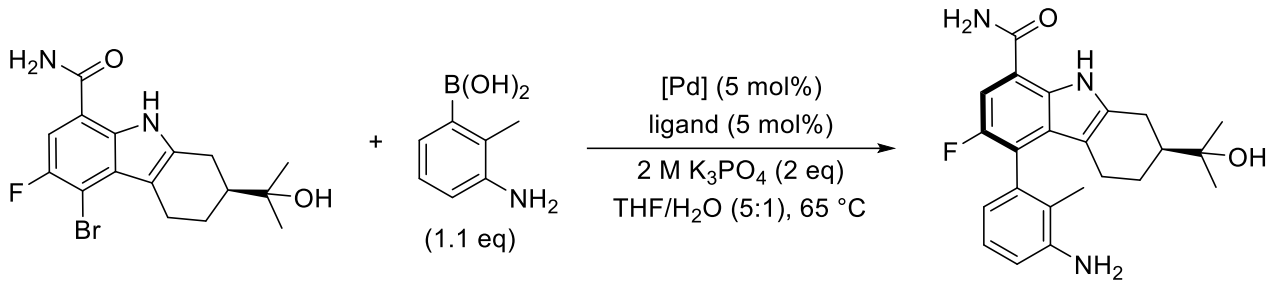

Metal/Ligand	Yield	dr
$PdCl_2$(dppf)	91.7	1.4:1
$Pd(OAc)_2$/(S)-Xyl-SDP	51.7	5.4:1
$Pd(OAc)_2$/(R)-BINAP	92.3	2.0:1

- (*R*)-BINAP was optimized despite (*S*)-Xyl-SDP higher selectivity ($230,000 /kg vs. $3,500 /kg respectively).
- The final process could run to 60 kg scale, with 87% yield, 14:1 dr, with crystallization from *n*-BuOH increased dr to 50:1.

Proof of Concept for Synthesis of BMS-986142

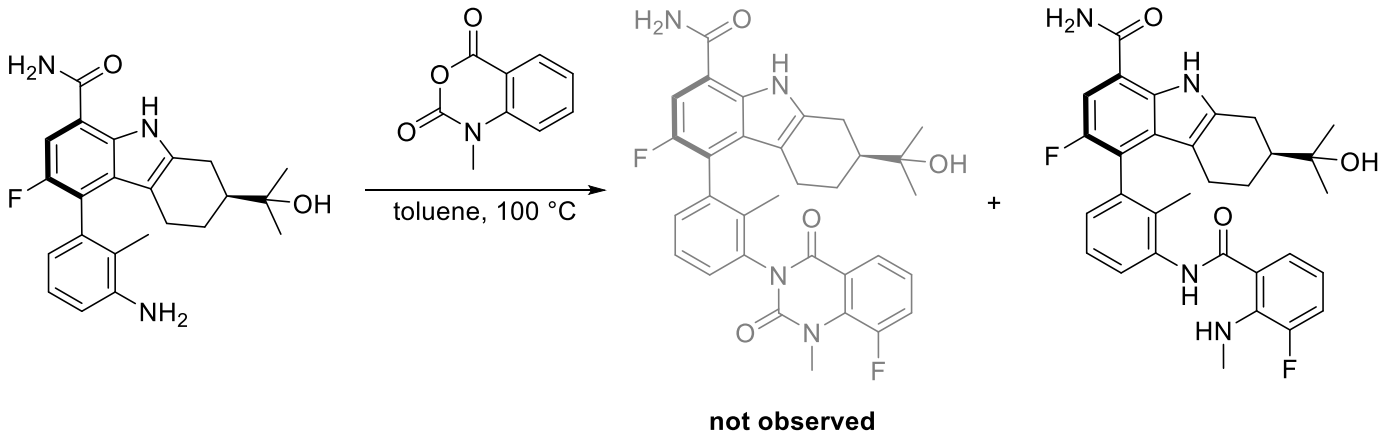

- Despite originally targeting a dynamic crystallization, this intermediate provided an available method to analyze the diastereoselectivity

Beutner *et al. Org. Lett.* **2018**, *59*, 9173–9200; Watterson, S. *et al. ACS Symposium Series*, Vol 1423, **2022**

Chirality Transfer in De Novo Synthesis: Designing an Optimal Route

Large Dependence of Carbamate R Group

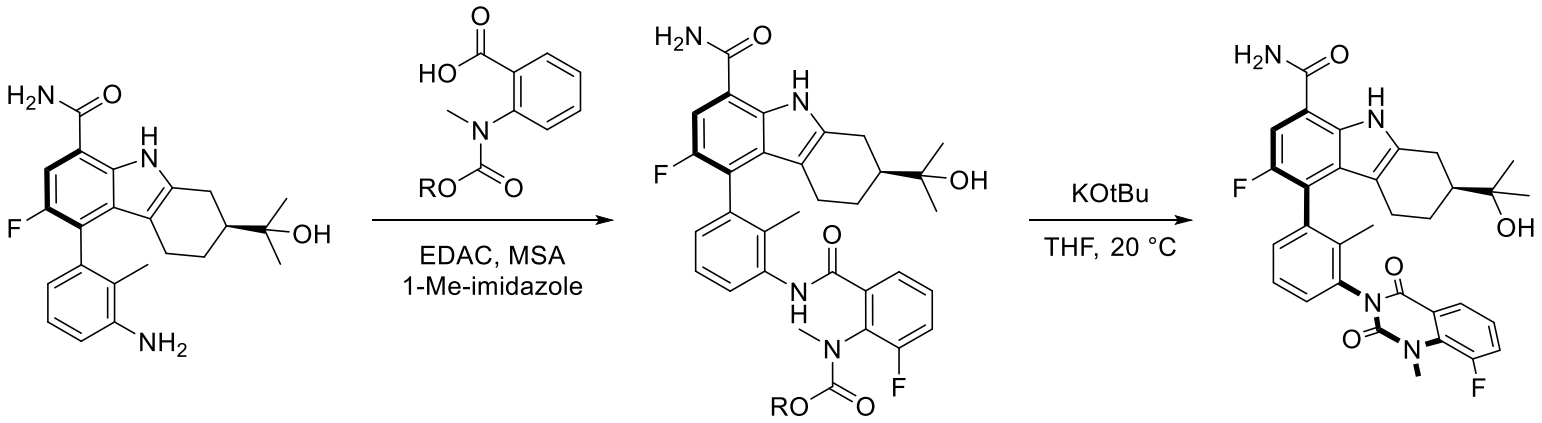

Carbamate R Group	dr
benzyl	2.7:1
phenyl	1:1.5
methyl	3.8:1
ethyl	5.0:1
n-propyl	6.0:1
isopropyl	4.7:1

Counterion and Solvent Dependencies

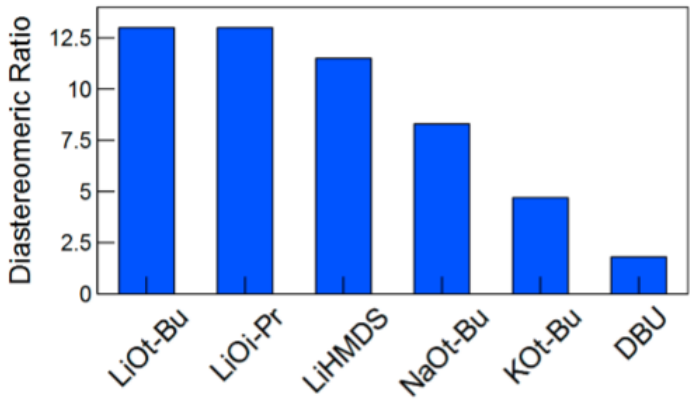

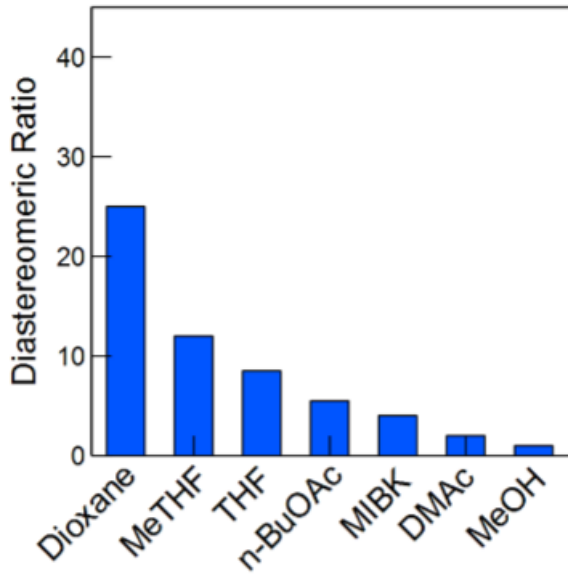

- $Li^+ > Na^+ > K^+$ in terms of diastereoselectivity
- Dioxane had the highest diasatereoselectivity, but was substituted with Me-THF

Beutner *et al. Org. Lett.* **2018**, *59*, 9173–9200; Watterson, S. *et al. ACS Symposium Series*, Vol 1423, **2022**: Wisniewski S. *Org. Process. Res. Dev.* **2018**, *22*, 1426-1431

Chirality Transfer in De Novo Synthesis: Designing an Optimal Route

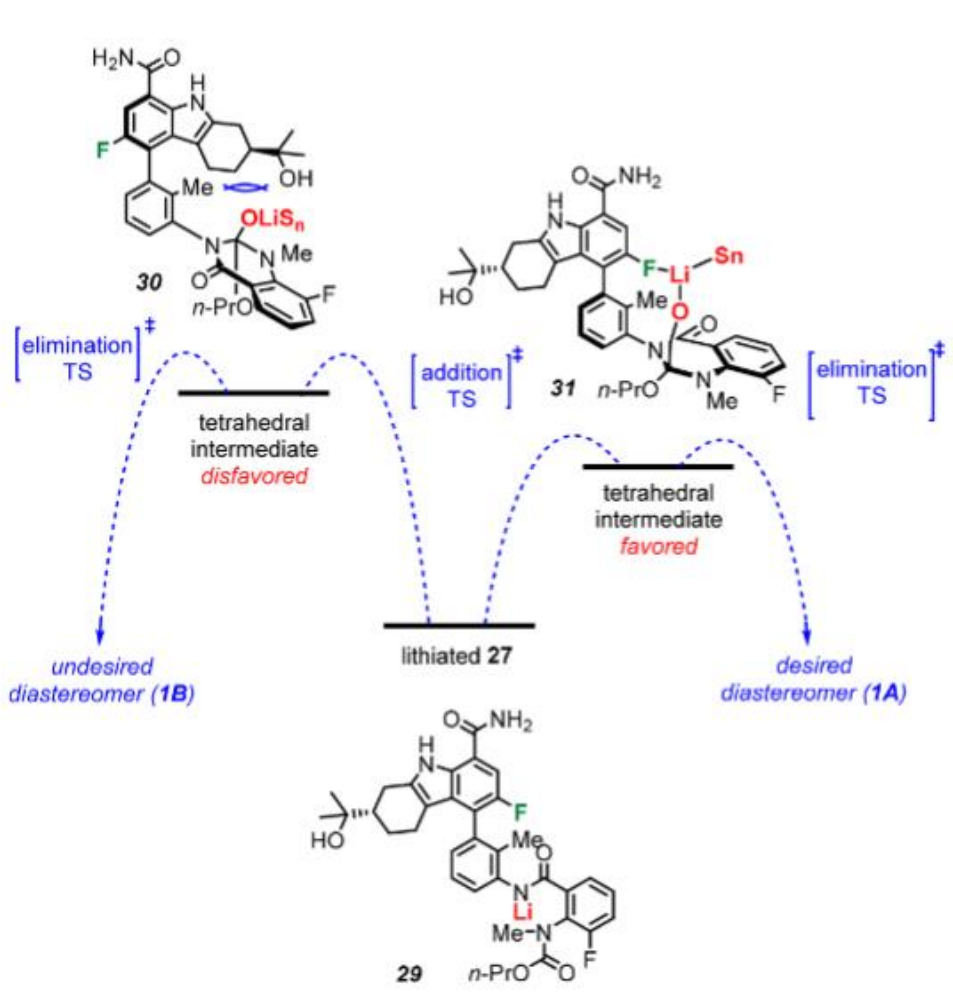

❖ "B3LYP modeling" showed steric interaction and preferred Li-F interaction

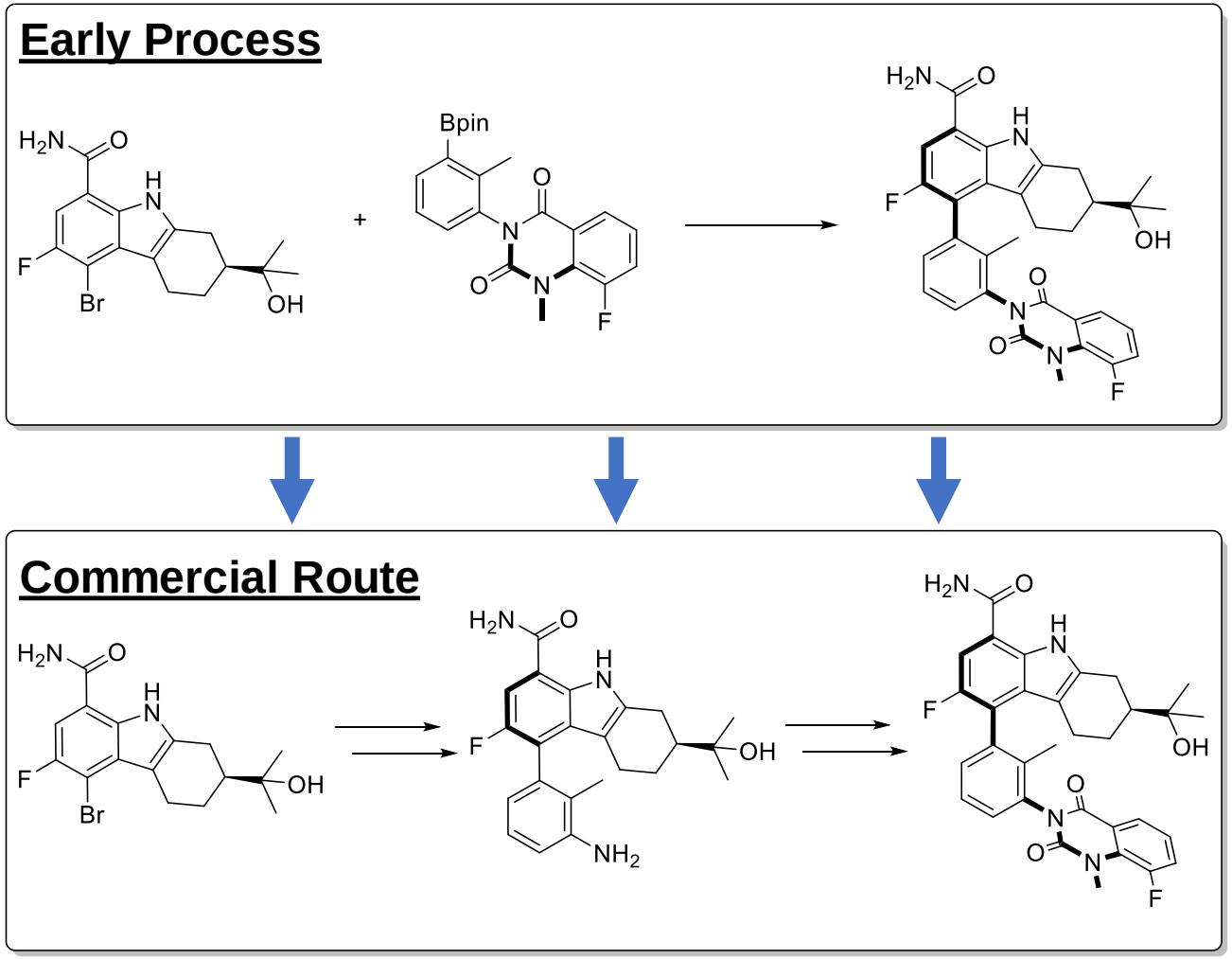

- Overall yield from 0.3% yield to 5.3 % yield
- Route PMI from 12798 to 691
- Total cycle time from 1205 h to 98 h

Beutner *et al. Org. Lett.* **2018**, *59*, 9173–9200; Watterson, S. *et al. ACS Symposium Series*, Vol 1423, **2022**

Summary

Chiral or Kinetic Resolution

- Operational simplicity allows for quick isolation of products in discovery
- Does not require significant optimization
- High PMI and maximum 50% yield
- Not scalable for process and commercialization

Functionalization or Dynamic Process

- Allows for chromatography-free creation of a single atropisomer
- Requires screening campaign to find optimal chiral reagent
- Depending on barrier of rotation, may require flow chemistry to decouple crystallization and racemization

Cross Coupling

- Allows for chromatography creation of a single atropisomer
- Often can be optimized up to high selectivity
- Often requires higher temperatures, preventing use with lower barrier atropisomers

De Novo Synthesis

- Can afford product in full yield without as many temperature restrictions
- Suffers from ligand optimization campaigns
- Higher risk due to possible unexpected reactivity and installation of functional handle

Summary

Considerations in Pharmaceutical Chemistry

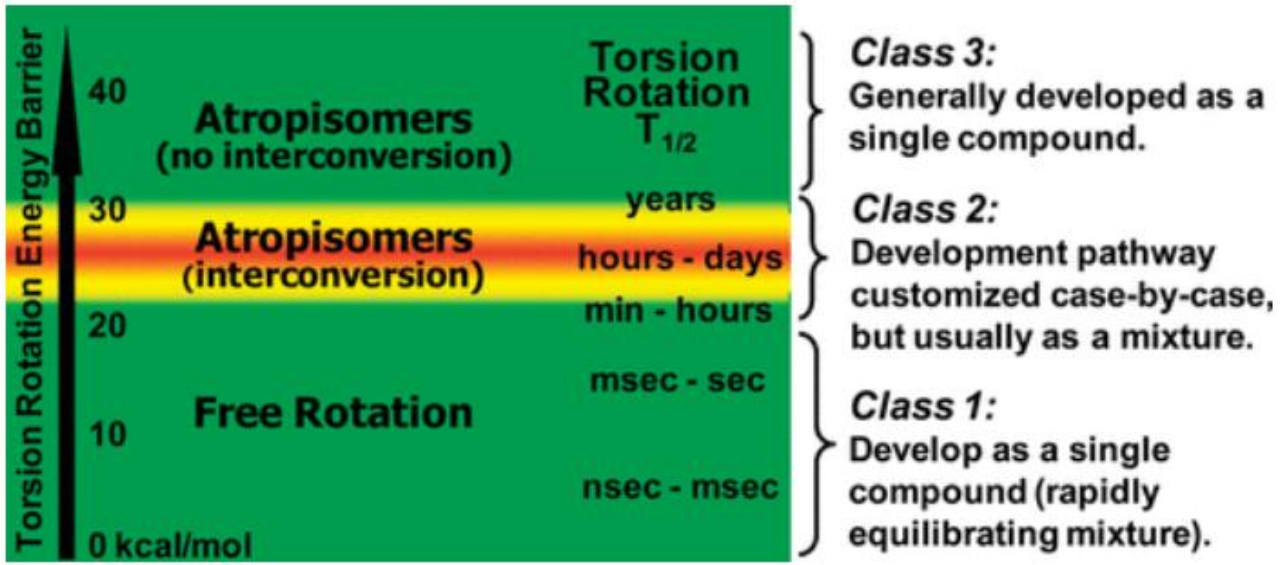

- Industry standard tends to bias towards **Class 1** atropisomer development
- **Class 3** atropisomers can help lock compounds into their bioactive conformation, making them more potent
- **Class 2** atropisomers are problematic due to potential access to other enantiomer

LaPlante, S.R. *et al. J. Med Chem.* **2011**, *54*, 7005-7022

Reviews of and Accounts of Interest

Stephane Perreault, Jayaraman Chandrasekhar, and Leena Patel
Atropisomerism in Drug Discovery: A Medicinal Chemistry Perspective Inspired by Atropisomeric Class I P13K Inhibitors
*Acc. Chem. Res.***2022**, *55*, 2581-2593

Xue Zhang, Kun Zhao, and Zhenua Gu
Transition Metal-Catalyzed Biaryl Atropisomer Synthesis via a Torsional Strain Promoted Ring-Opening Reaction
Acc. Chem. Res. **2022**, *55*, 1620-1633

Steven R. LaPlante *et al.*
Assessing Atropisomer Axial Chirality in Drug Discovery and Development
J. Med Chem. **2011**, 54, 20, 7005-7022

Casey B. Roos *et al.*
Stereodenyamic Strategies to Induce and Enrich Chirality of Atropisomers at a Late Stage
Chem. Rev. **2023**, *123*, 10641-10727

Mariami Basilaia, Matthew H. Chen, Jim Secka, and Jeffrey L. Gustafson
Atropisomerism in the Pharmaceutically Relevant Realm
Acc. Chem. Res. **2022**, *55*, 2904-2919

Questions?

Outline

I. Atropisomerism and Motivations in Pharmaceuticals

II. Methods of Formation:

   I. Case Study 1: Classic Resolution to Dynamic Resolution

   II. Case Study 2: Cross-Coupling

   III. Case Study 3: De Novo Ring Synthesis

De Novo Synthesis Case Study: Scaling the Reaction

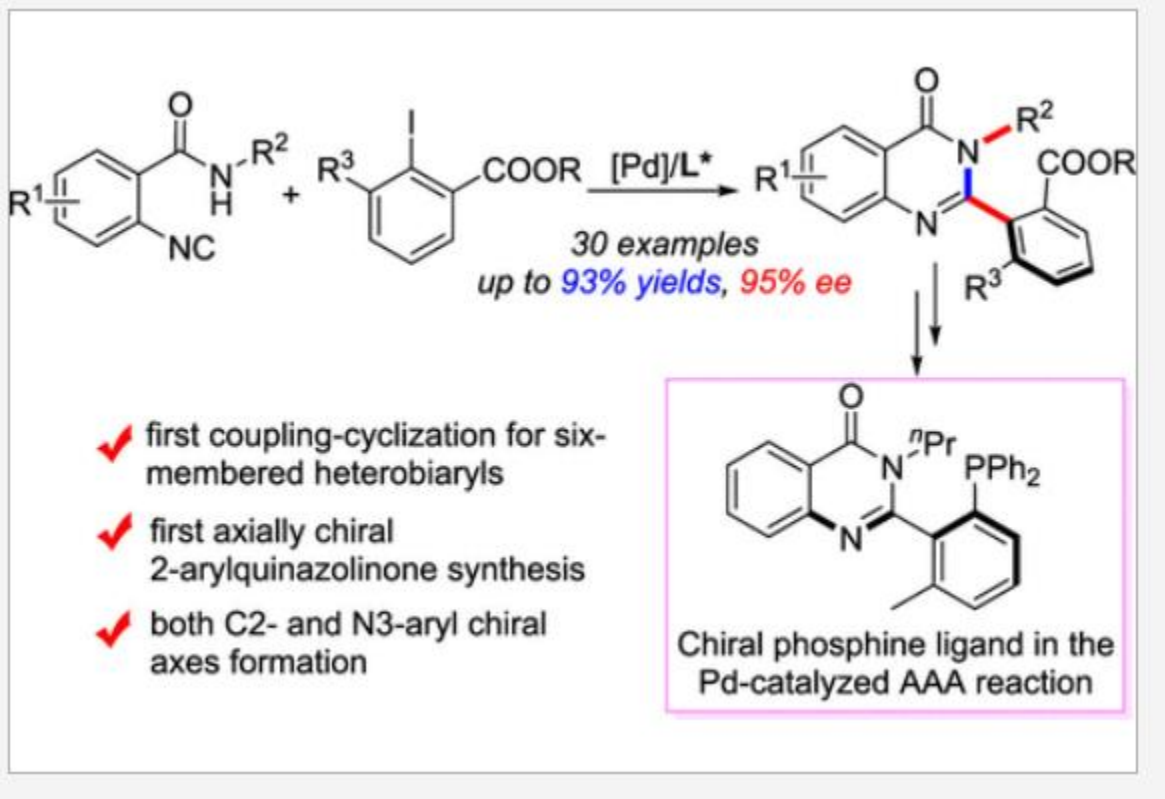

J. Am. Chem. Soc. 2021, 143, 7, 2722–2728

Synthesis of Astrazeneca NK1 Inhibitor

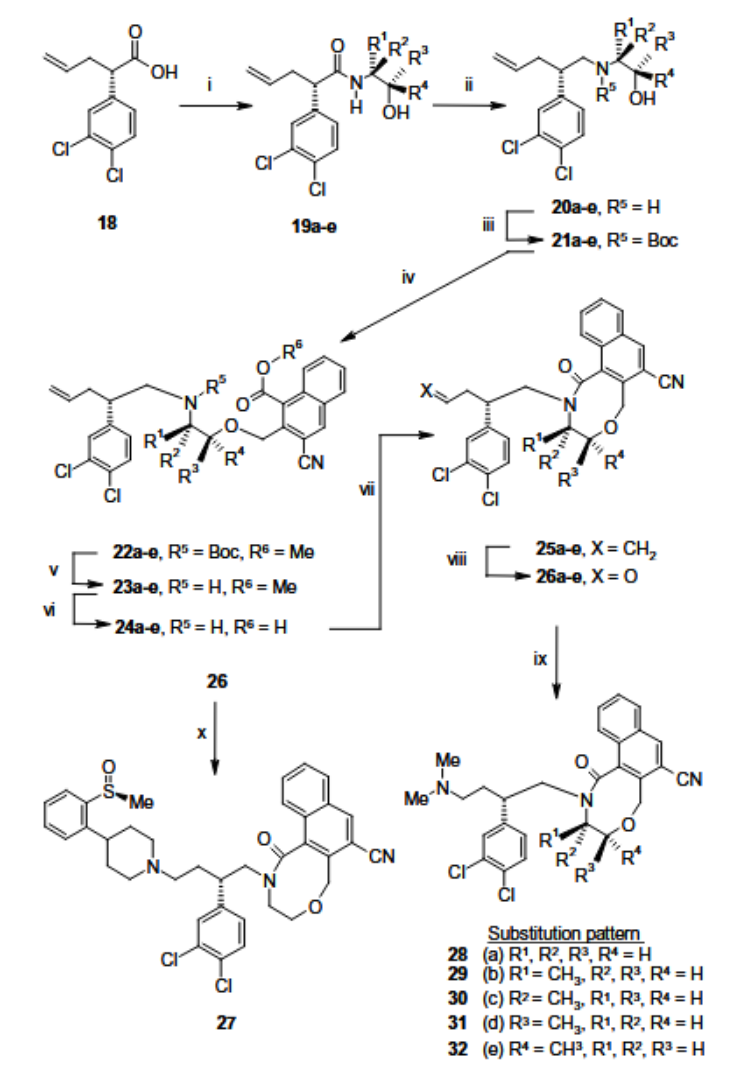

Scheme 1. (i) 3-Cyano-2-methoxy-1-naphthoyl chloride, NaOH, CH_2Cl_2; (ii) *t*BuMe$_2$SiCl, DMAP, Et_3N, CH_2Cl_2; (iii) MgI_2, benzene; H_2O; (iv) Cl(CH$_2$)$_{2\text{-}3}$OH, DMF, K_2CO_3; (v) $MeSO_2Cl$, Et_3N, CH_2Cl_2; (vi) NaH, THF; (vii) 5% HF/MeCN; (viii) trioxane, HOAc, H_2SO_4, CH_2Cl_2; (ix) 1 N NaOH, THF, MeOH, (x) oxalyl chloride, DMSO, Et_3N, CH_2Cl_2; (xi) 4-[(*S*)-2-methylsulfinylphenyl]piperidine, $NaBH_4$, HOAc, MeOH.

Scheme 2. (i) *i*Pr$_2$EtN, H$_2$NCR^{1}R^{2}CR^{3}R^{4}OH, DMAP, Me$_2$NCH$_2$-CH$_2$CH$_2$N=C=NEt·HCl; (ii) $LiAlH_4$, Et_2O; (iii) O(CO$_2$*t*-Bu)$_2$, Na_2CO_3, dioxane/H_2O; (iv) NaH, methyl 2-(bromomethyl)-3-cyano-1-naphthoate, **33**, DMF, THF; (v) TFA, CH_2Cl_2; (vi) pyridine hydrochloride, 180 °C; (vii) BOP-Cl, *i*Pr$_2$EtN, MeCN, (viii) O_3, CH_2Cl_2, −78 °C, Me$_2$S; (ix) Me$_2$NH·HCl, HOAc, $NaBH_3CN$, MeOH; (x) 4-[(*S*)-2-methylsulfinylphenyl]piperidine, HOAc, $NaBH_3CN$, MeOH.

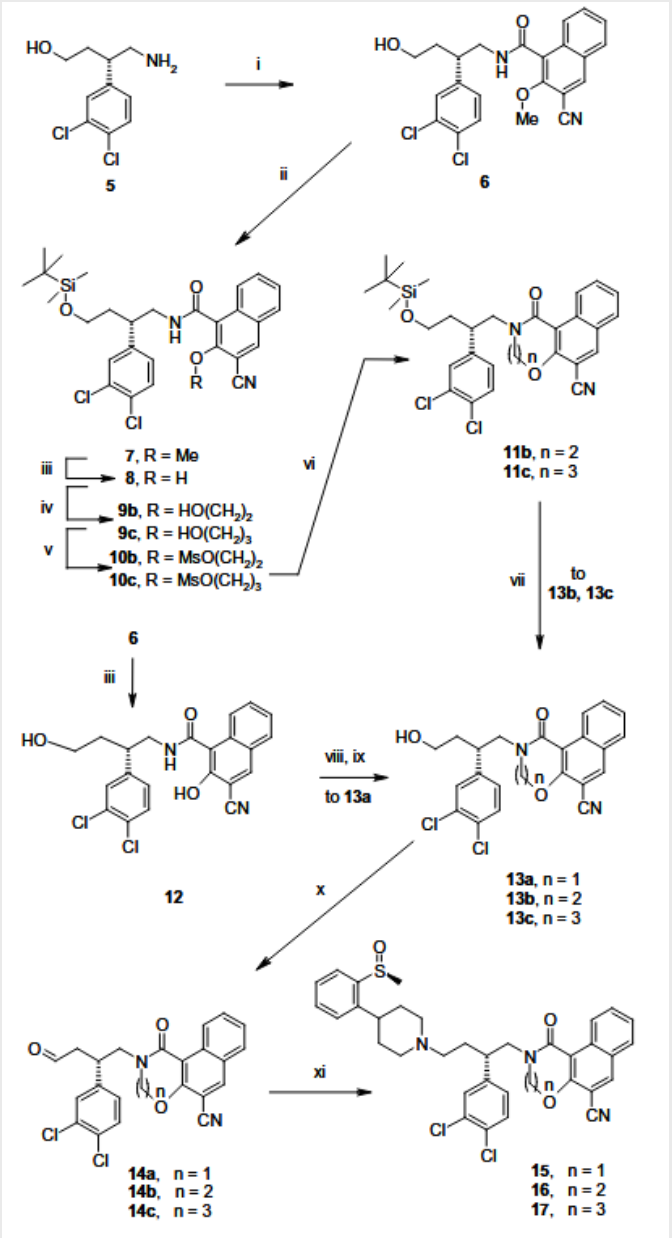

Ohnmacht J. *et al. Bioorg. Med. Chem.* **2004**, *12*, 2653-2669

Atropisomeric Configurational Stability Assessment

Table 2. Choosing an Experimental Technique for Configurational Stability Assessment

Technique	Favored by	Disfavored when	Compound requirement
VT-NMR: Line-shape analysis, EXSY, or kinetic analyses	Fast interconversion ($t_{1/2}$ < 1 s,[26] e.g., analysis of non-chromatographically separable isomer mixtures), $\Delta G^{\ddagger}$ < 23 kcal/mol[27]	Atropisomers are enantiomers or chemically unstable at elevated temperature	~3 mg of atropisomer mixture (or atropisomerically enriched material)
Time-course NMR	Medium-to-slow interconversion within the accessible temperature rage ($t_{1/2}$ > 5 min[23]), $\Delta G^{\ddagger}$ = 22–33 kcal/mol[28]	Atropisomers are enantiomers or unstable, chiral separation is not feasible	~3 mg of atropisomerically enriched material
Chiral Chromatography (e.g., HPLC, SFC)	Slow interconversion ($t_{1/2}$ > 20 min[23]), $\Delta G^{\ddagger}$ > 24 kcal/mol	Atropisomers are rapidly converting, or chiral separation is not feasible	<1 mg of atropisomerically enriched material

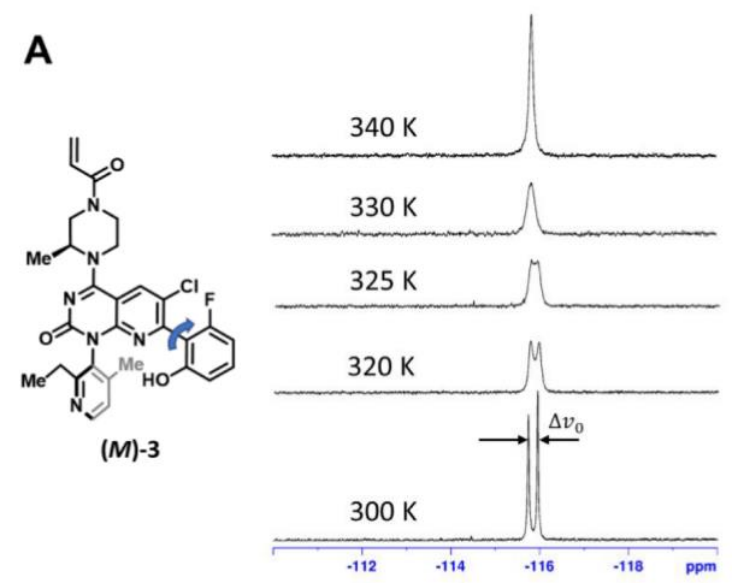

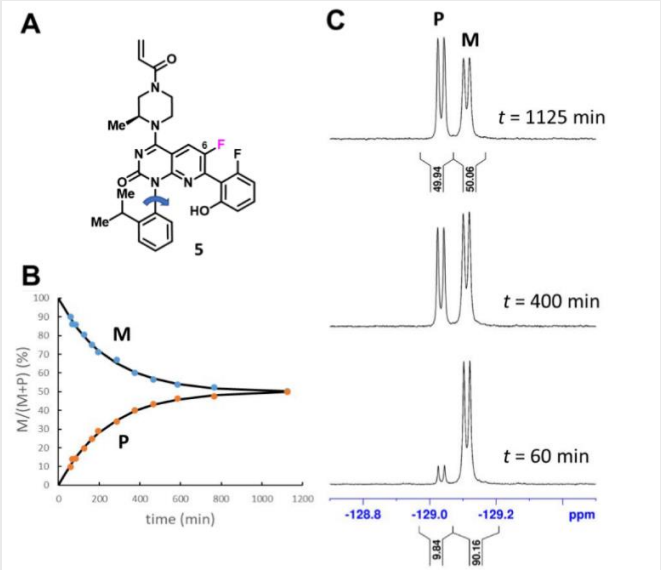

Lanman *et al. Acc. Chem. Res.* **2020**, *55*, 2892-2903;

Sotorasib

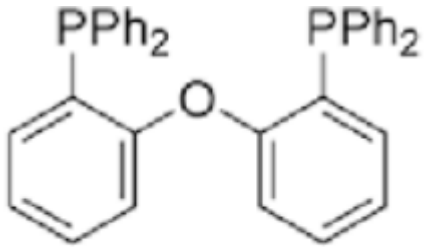

DPEphos

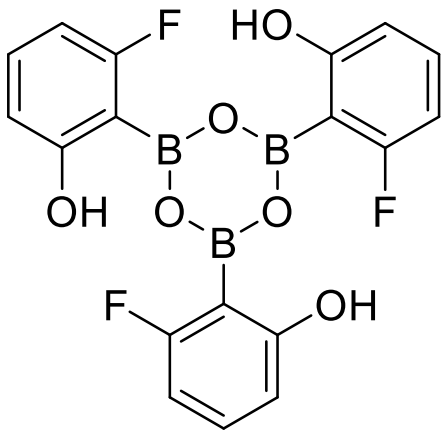

Lanman *et al. Acc. Chem. Res.* **2020**, *55*, 2892-2903;

Calculation of barrier

$$e.r. = \frac{k_{maj}}{k_{min}}$$

$$k = \frac{\kappa h}{k_B T} e^{-\left(\frac{\Delta G^{\ddagger}}{RT}\right)} 1$$

$$\ln(e.r.) = \left(\frac{-1}{RT}\right)\left(\Delta G^{\ddagger}_{maj} - \Delta G^{\ddagger}_{min}\right) = \left(\frac{-1}{RT}\right)\left(\Delta\Delta G^{\ddagger}\right)$$

$$\Delta\Delta G = -RTln(e.r.)$$

Lanman *et al. Acc. Chem. Res.* **2020**, *55*, 2892-2903;

Sotorasib

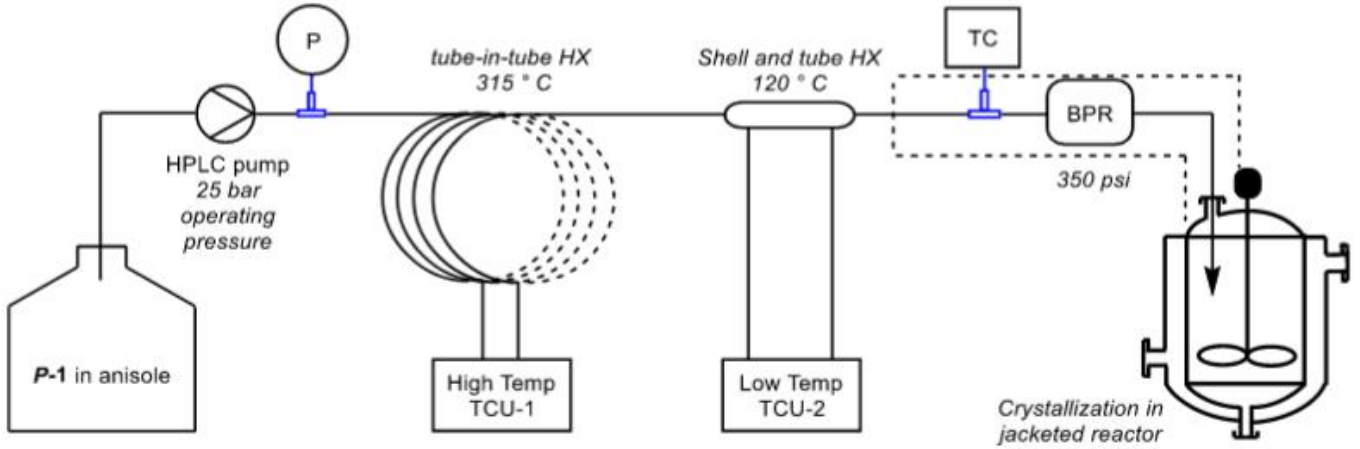

Figure 5. Process flow diagram for the lab-scale PFR system.

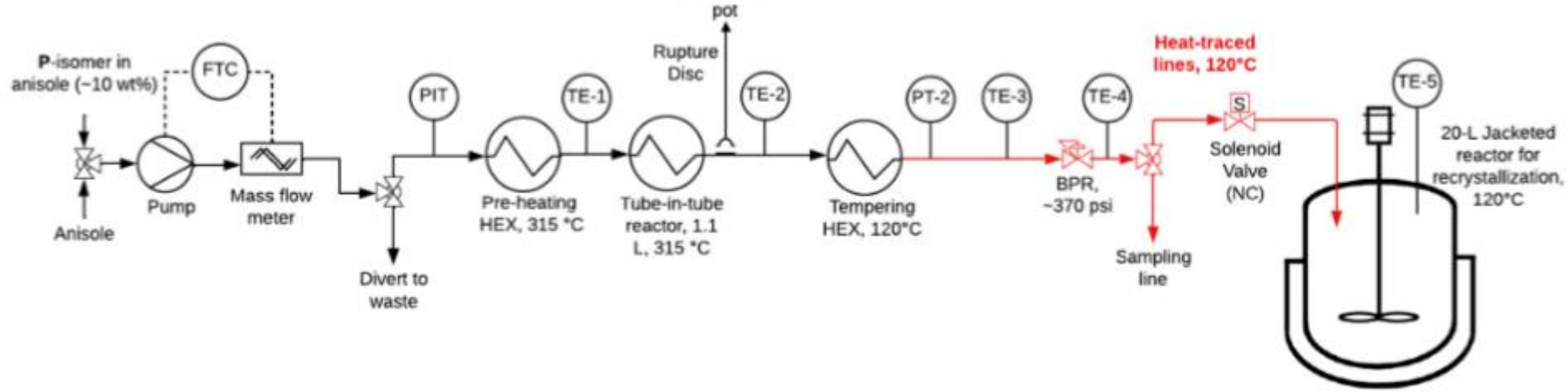

Lanman *et al. Acc. Chem. Res.* **2020**, *55*, 2892-2903;

First Generation Synthetic Route Towards GDC-6036

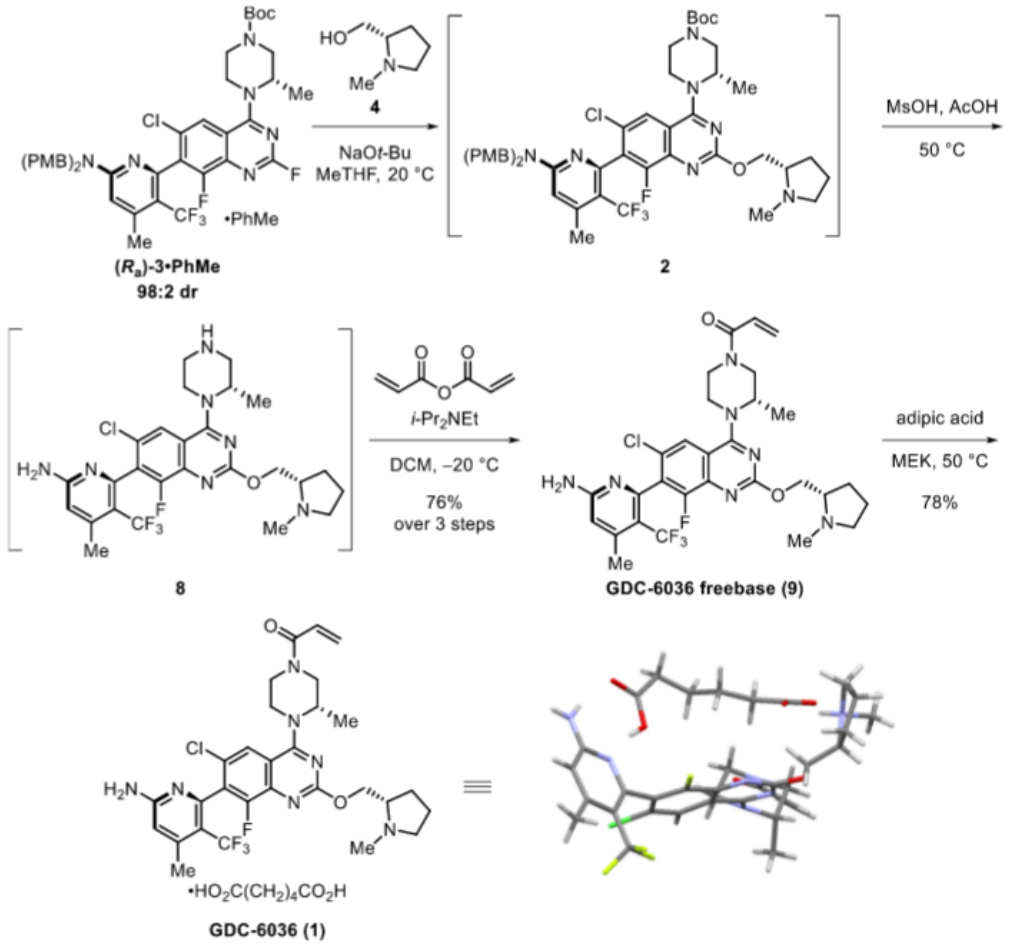

Xu *et al. J. Am. Chem. Soc.* **2022**, 144, 20955-20965

Other Results in Chemoinformatic Workflow

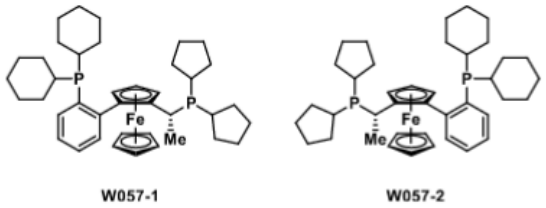

Table 2. Scope of the Negishi Coupling Employing W057-2

Entry[a]	Product	Conv (%)[b]	Yield (%)[c]	*er*[b]
1	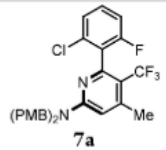 **7a**	12	3	88:12
2	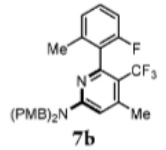 **7b**	24	8	75:25
3	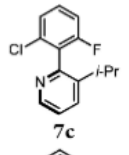 **7c**	37	25	74:26
4	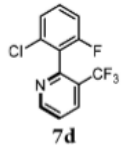 **7d**	72	59	60:40
5	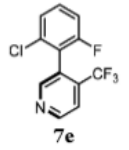 **7e**	31	16	79:21

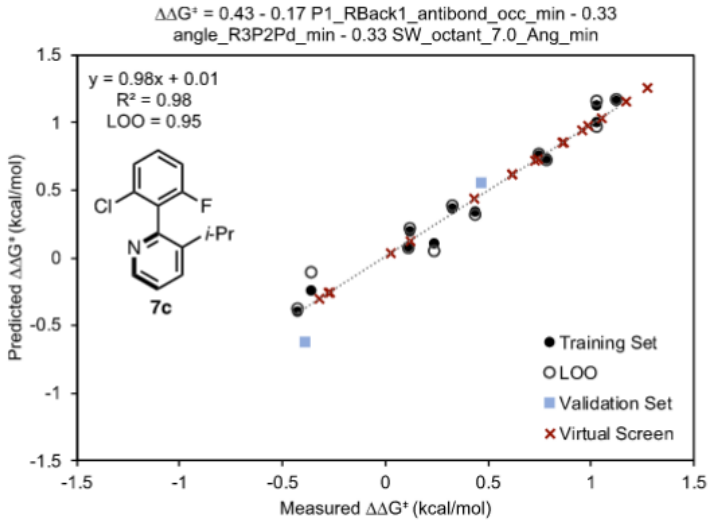

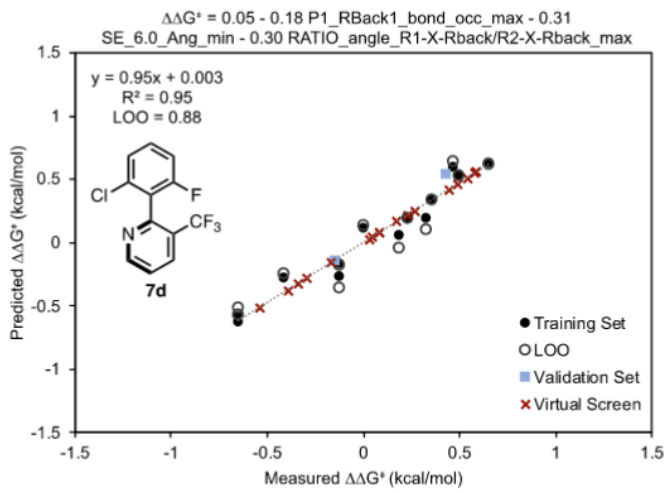

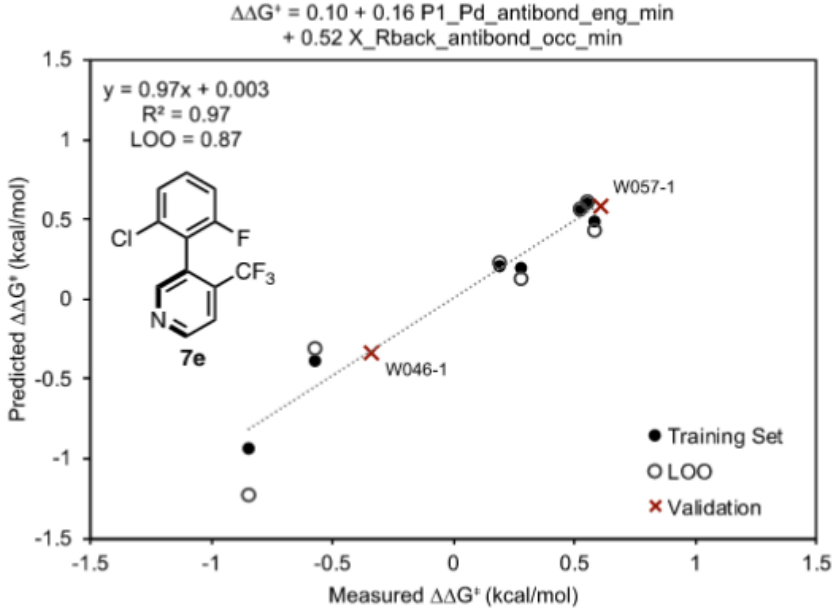

Xu *et al. J. Am. Chem. Soc.* **2022**, 144, 20955-20965

Second Generation Route

Scheme 2. Concise Synthesis of Aminopyridine 5

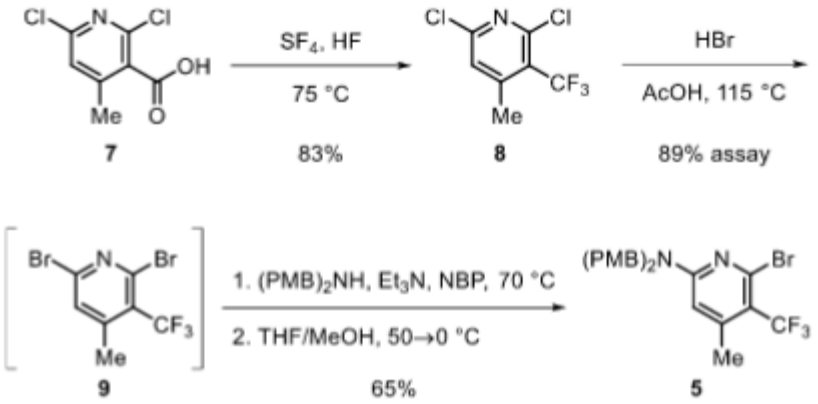

Scheme 3. Synthesis of Quinazoline 6

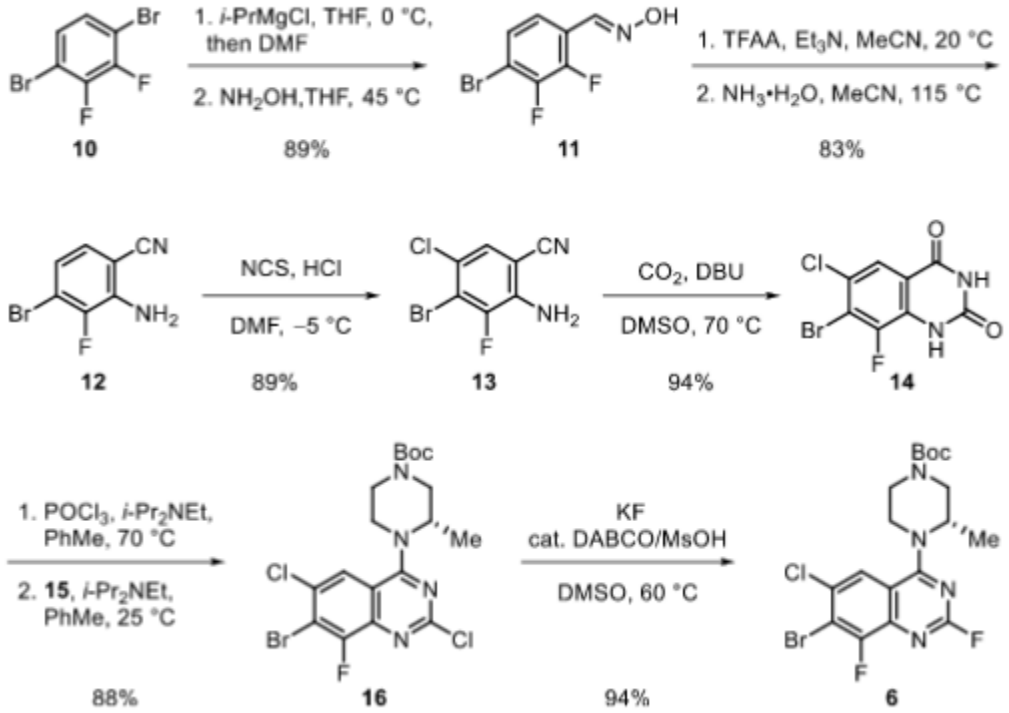

Xu *et al. Org. Lett.* **2022**, 144, 20955-20965

Second Generation Route

Scheme 5. Endgame of the Synthesis of GDC-6036 (1)

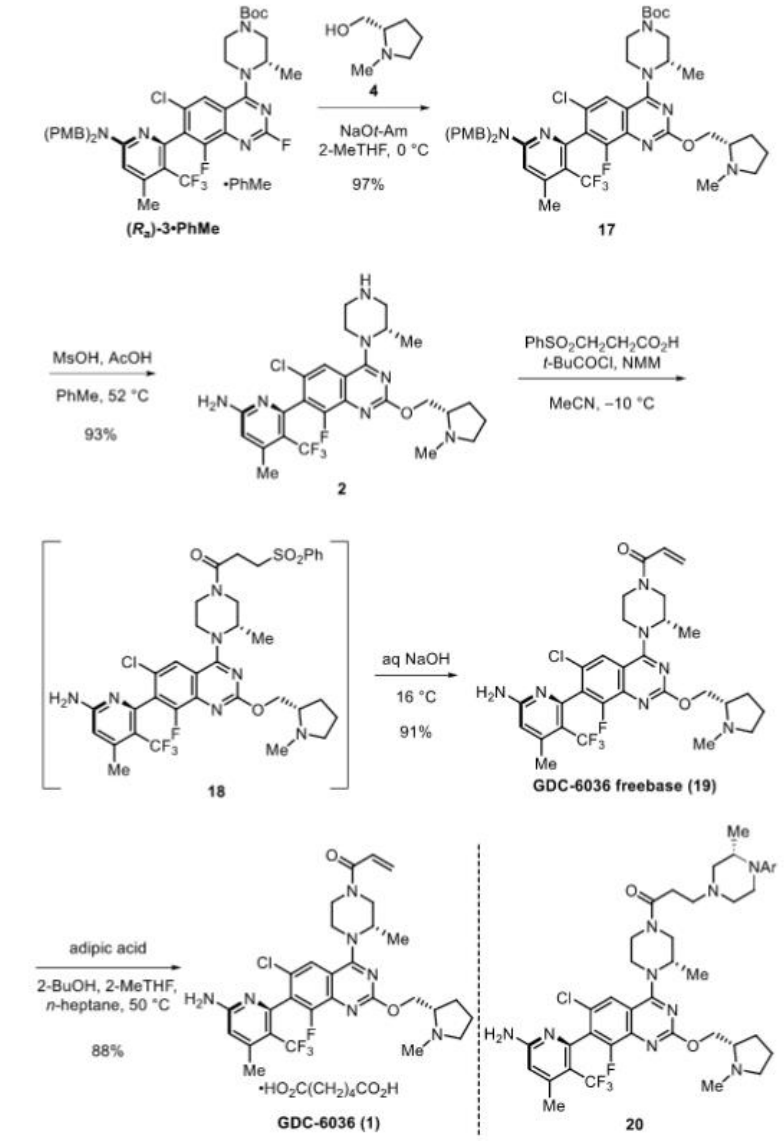

Xu *et al. Org. Lett.* **2022**, 144, 20955-20965

Full Med Chem Route to BMS-986142

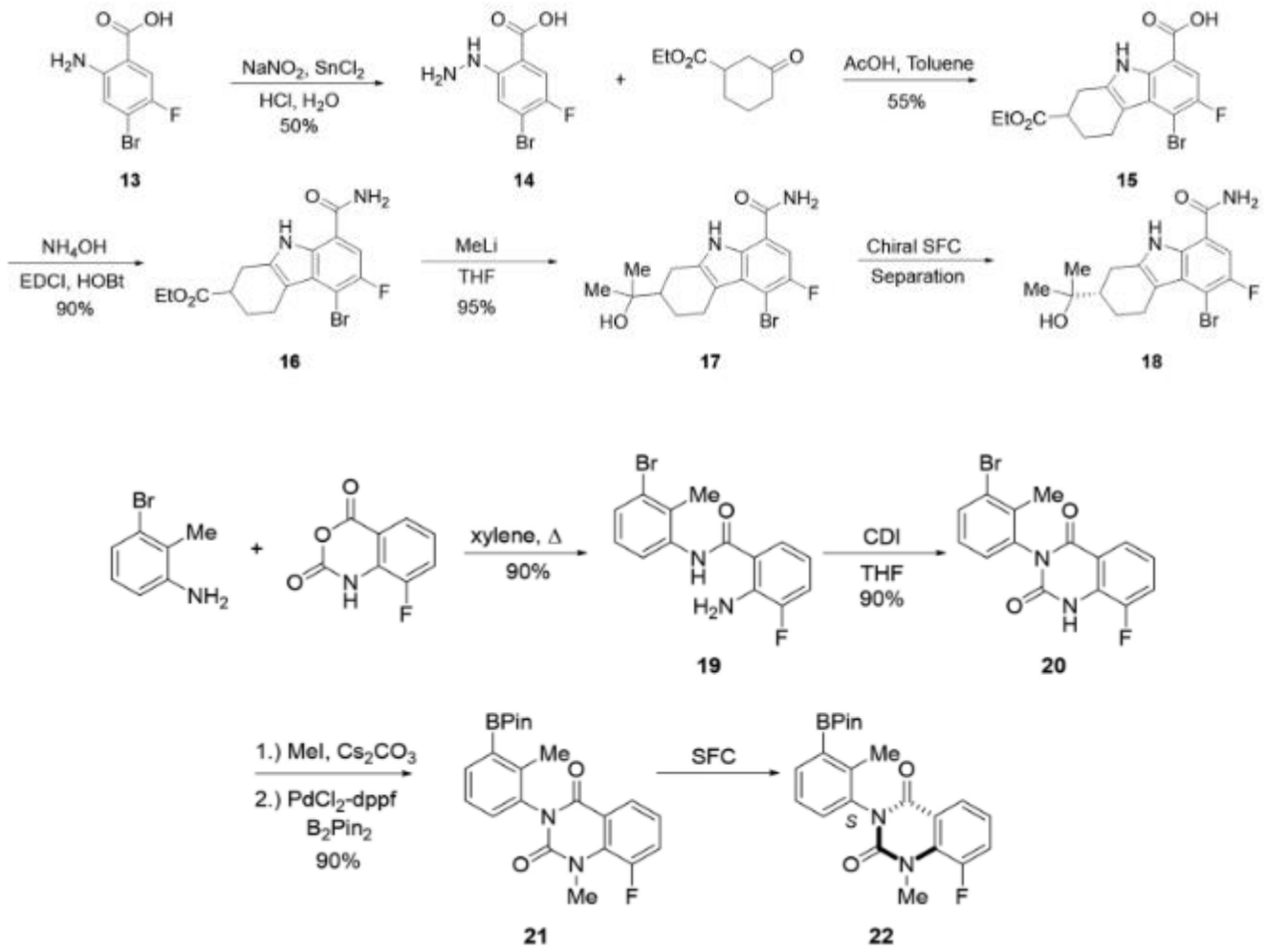

Watterson, S. *et al. ACS Symposium Series*, Vol 1423, **2022**

Phosphine Oxide Steps

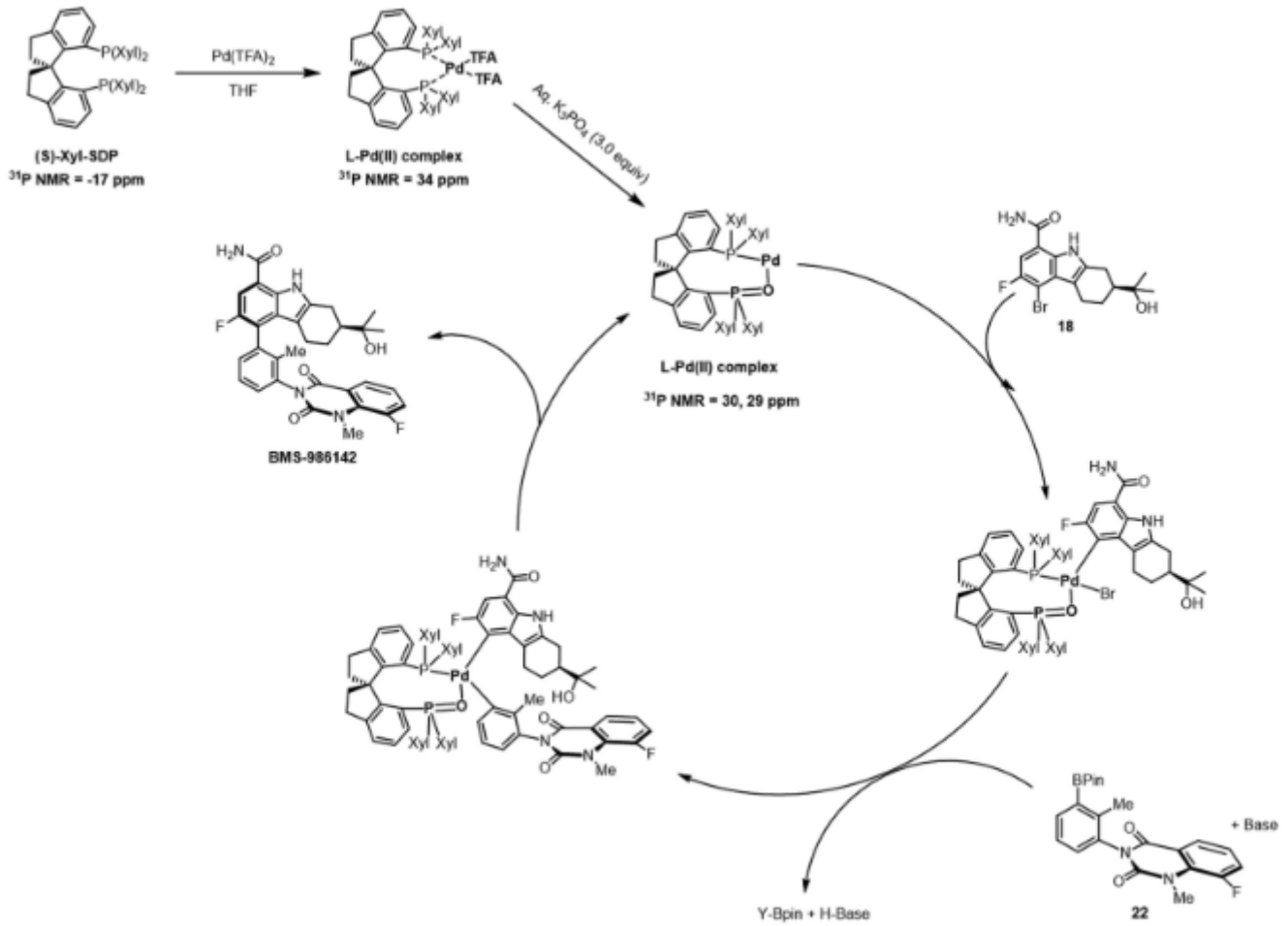

Scheme 7. Catalyst activation with (S)-Xyl-SDP.

Watterson, S. *et al. ACS Symposium Series*, Vol 1423, **2022**

Suzuki-Miyaura Final Process

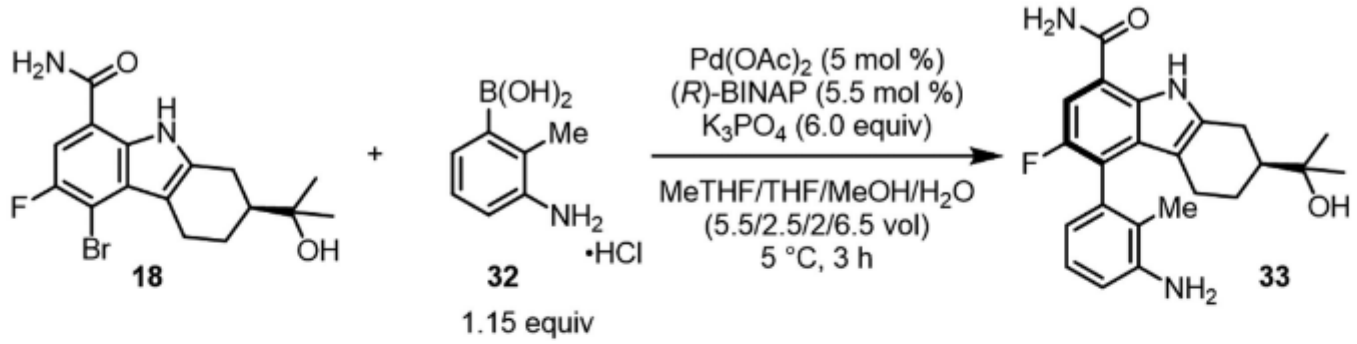

Impurities:

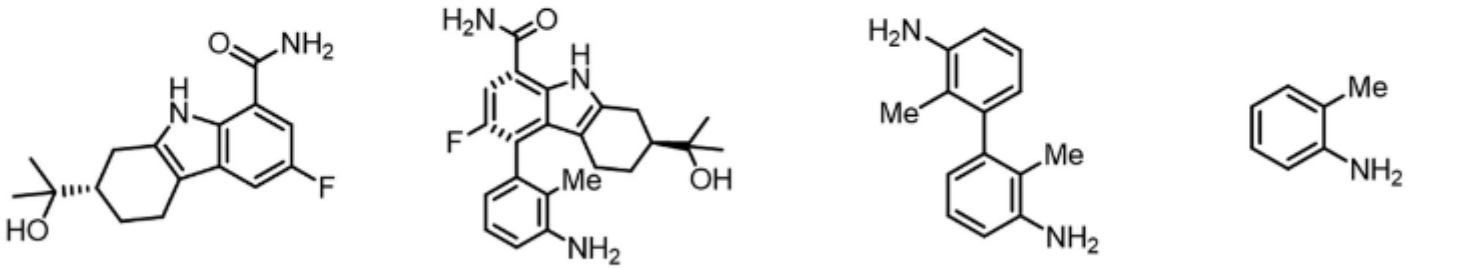

Dehalogenation
In-process: 0.5-0.7%
Isolated: 0.05-0.09%

Other Atropisomer
In-process: 6.1-6.9%
Isolated: 1.1-1.6%

Boronic Acid Dimer
In-process: 0.2-0.05%
Isolated: ND

Protodeboronation
In-process: 0.1-0.7%
Isolated: ND

Scheme 14. Optimization of Suzuki-Miyaura reaction and on-scale performance.

Watterson, S. *et al. ACS Symposium Series*, Vol 1423, **2022**

Dynamic Kinetic Resolution Case Study: MRTX1719 and PRMT5•MTA

Targeting PRMT5•MTA for Cancer Suppression

- PRMT5 is a protein arginine methyltransferase that adds two methyl groups to arginines of it substrate protein
  - This binds to methylosome protein 50 (MEP50), which plays an essential role in cell survival
- Methylthioadenosine phosphorylase (MTAP) gene deletion is often co-deleted with tumor suppressor genes
  - This causes both higher dependence on PRMT5 and build up of MTA, which inhibits PRMT5
- MRTX1719 targets the PRMT5 complex in MTAP-missing cells, preventing targeting of normal cells

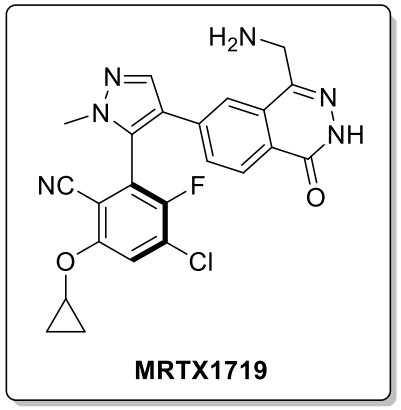

MRTX1719

Crystal Structure of MRTX1719 with PRMT5•MTA

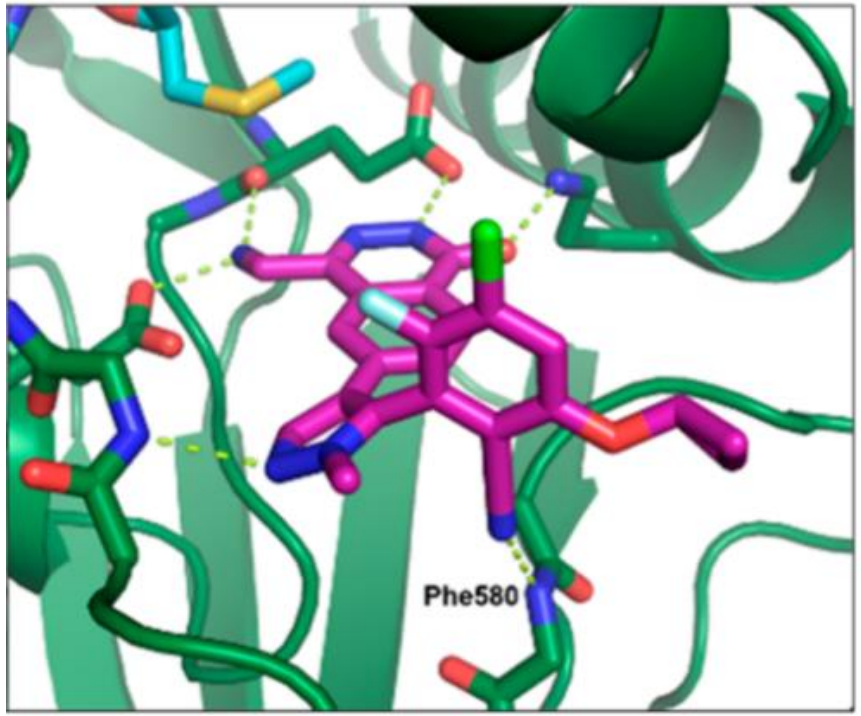

- Key Interactions:
  - Aryl nitrile makes a favorable H-bond with Phe580
  - The pyrazole interacts with Leu312
  - Phthalazinone interacts with Glu435 and Lys333

Smith *et al. J. Med. Chem.* **2022**, *65*, 1749–1766

Dynamic Kinetic Resolution Case Study :

Initial Discovery Cross Coupling to Resolution

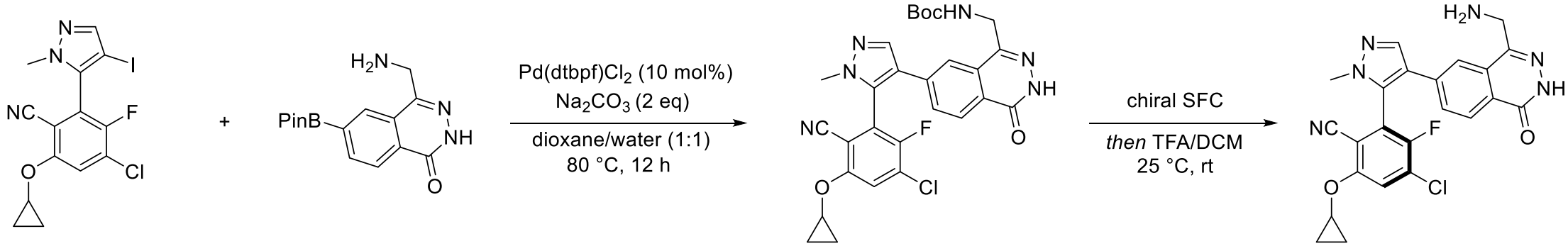

43% yield in 6 steps + **21% yield in 7 steps** → **74% yield** → **39% yield**

The Problem with Atropselective Cross Coupling

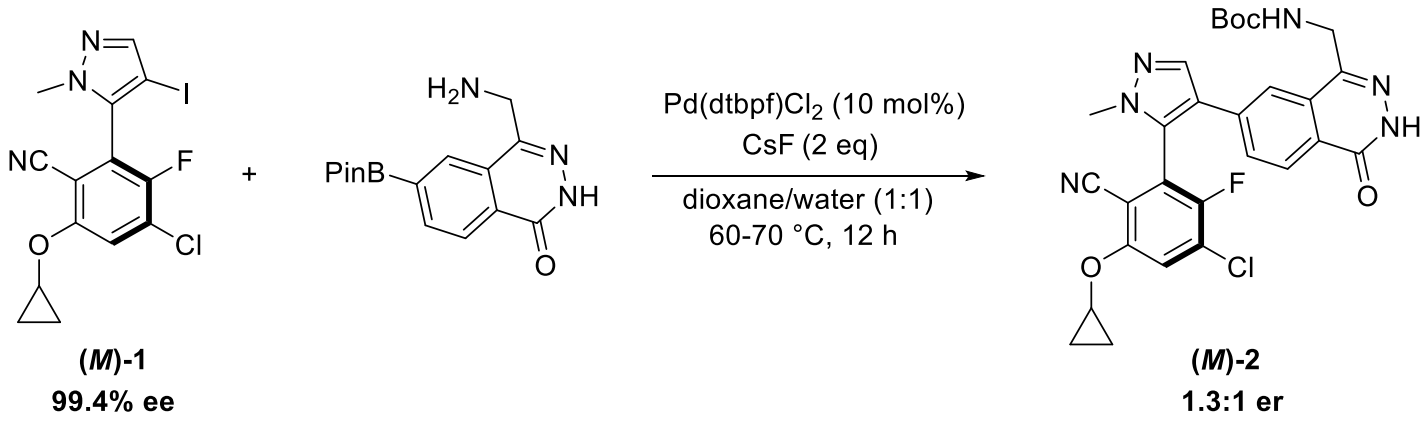

(*M*)-1
99.4% ee

(*M*)-2
1.3:1 er

- MRTX1719 has a 28.93 kcal/mol barrier at 25 °C
- (*M*)-1 only undergoed 0.8% ee loss at 80 °C, 8.1% ee at 100 °C
- (*M*)-2 has a higher racemization rate than (M)-1
  - This ruled out asymmetric cross-coupling approaches

Achmatowicz *et al. Org. Process Res. Dev.* **2023**, *27*, 954-971

Amidation Final Process

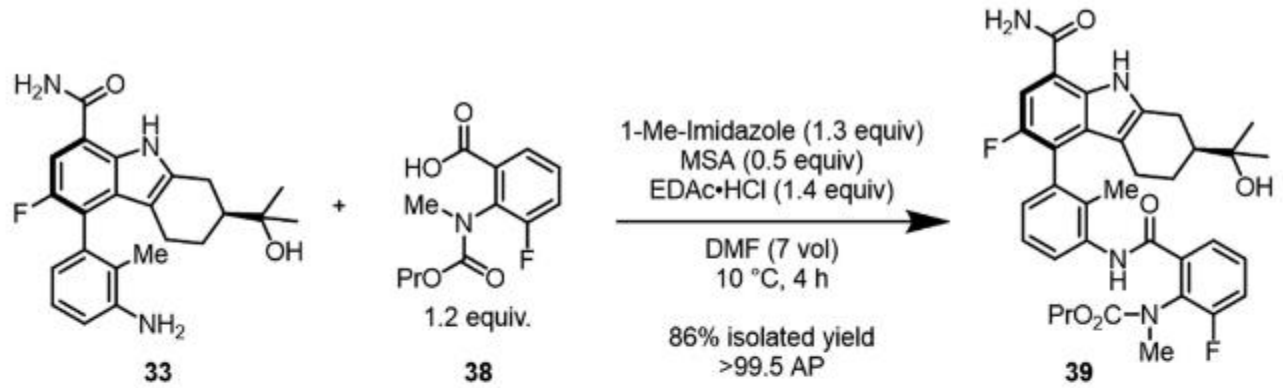

Impurities:

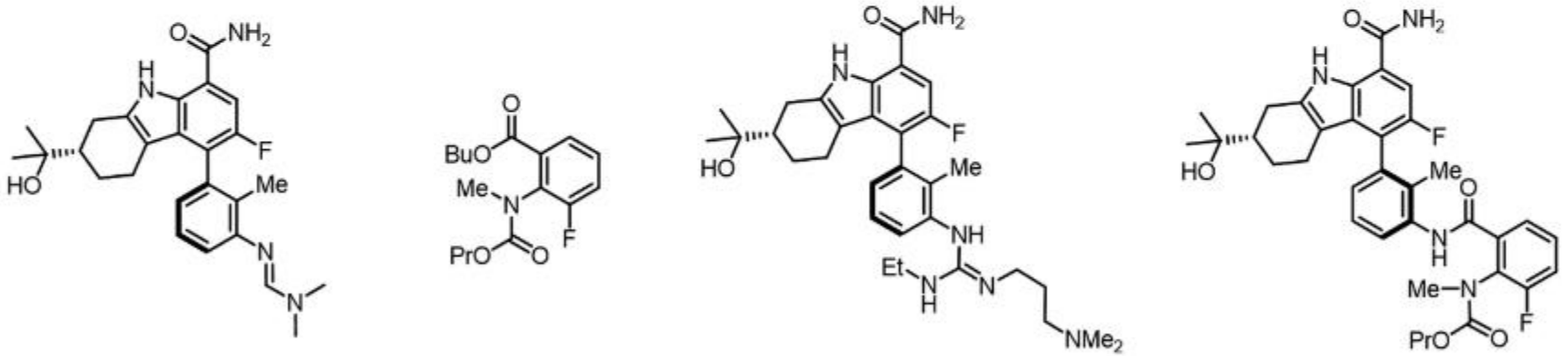

DMF Adduct
In-Process: ~2.0 AP
Isolated: ND

Butyl Ester
In-Process: 0-0.2 AP
Isolated: ND

EDAC Adduct
In-Process: ~1.3 AP
Isolated: ND

Other Atropisomer
In-Process: 1.1-1.6 AP
Isolated: 0.3-0.4 AP

Scheme 19. Impurities observed in the penultimate amidation.

Watterson, S. *et al. ACS Symposium Series*, Vol 1423, **2022**

Initial Med Chem Route MRTX1719

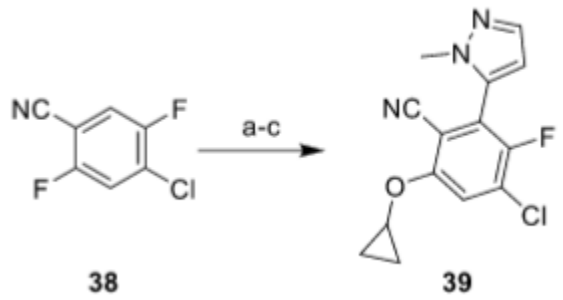

38 39

[a]Reagents and conditions: (a) Cyclopropanol (1.0 equiv), NaH, (1.05 equiv), THF, 60 °C, 1 h. (b) LDA (1.3 equiv), I_2 (2.0 equiv), THF, −78 to 25 °C, 12 h. (c) 1-Methyl-5-(4,4,5,5-tetramethyl-1,3,2-dioxaborolan-2-yl)-1*H*-pyrazole (1.4 equiv), Pd(dtbpf)Cl_2 (0.1 equiv), Na_2CO_3 (2 equiv), dioxane/water, 80 °C, 12 h.

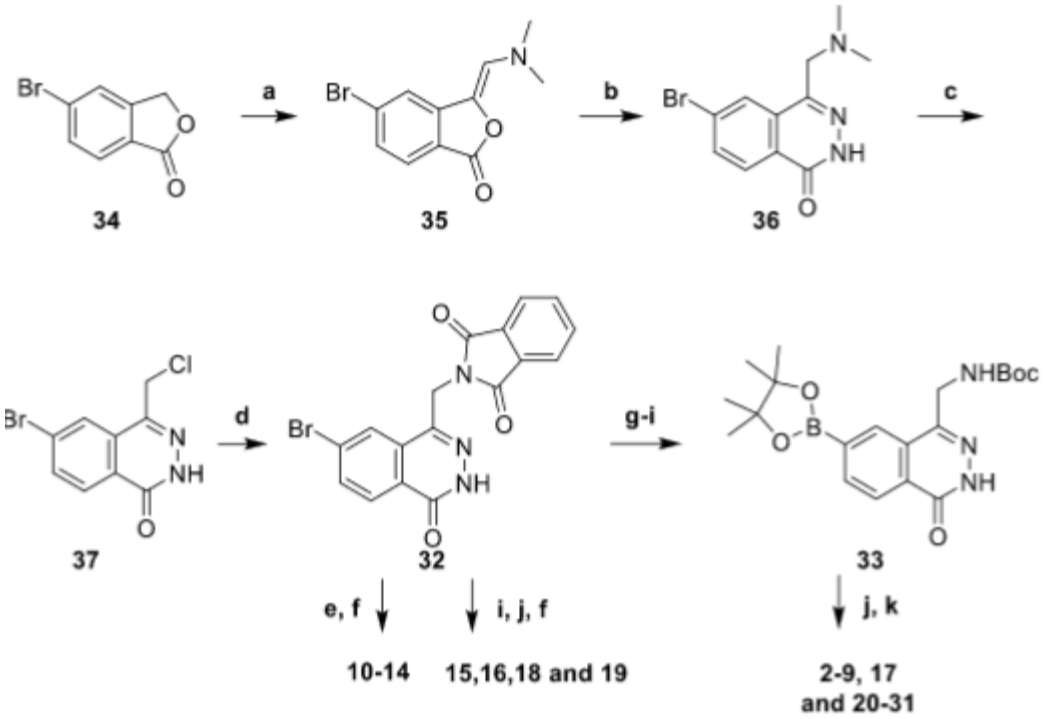

[a]Reagents and conditions: (a) DMF-DMA (6.44 equiv), ^{t}BuOK (0.10 equiv), 110 °C, 20 h. (b) Hydrazine hydrate (2.05 equiv), EtOH, 70 °C, 12 h. (c) Isobutyl chloroformate (1.20 equiv), THF, 25 °C, 6 h. (d) Potassium phthalimide (1.10 equiv), DMF, 25 °C, 1 h. (e) R_1-Bpin (1.5 equiv), Pd(dppf)Cl_2 (0.10 equiv), or Pd(dtbpf)Cl_2 (0.10 equiv), Na_2CO_3 (2.0 equiv), dioxane/H_2O, 80 °C, 2 h. (f) Hydrazine hydrate (1.00 equiv), EtOH, 80 °C, 1 h. (g) Hydrazine hydrate (1.00 equiv), EtOH, 80 °C, 16 h. (h) $(Boc)_2O$ (2.00 equiv), TEA (3.00 equiv), DCM, 25 °C, 16 h. (i) Bis(pinacolato)diboron (1.5 equiv), Pd(dppf)Cl_2 (0.10 equiv), KOAc (3.00 equiv), dioxane, 100 °C, 2 h. (j) (1) R_1-Hal (1.0 equiv), Suzuki Pd catalysts (0.1 equiv), Na_2CO_3 (2.0 equiv), dioxane/water, 80 °C, 2 h; (2) SFC separation of atropisomers if required. (k) TFA/DCM, 20 °C or HCl/MeOH, 0 °C, 0.5 h.

Smith *et al. J. Med. Chem.* **2022**, *65*, 1749–1766